MATERIALS AND METHODS

Reagents. Recombinant human IFN-α2b was from Schering-Plough (Kenilworth, NJ). Beta-mercaptoethanol was from Wako (Osaka, Japan). Antibodies used were SOCS3 and SOCS1, which were from Cell Signaling (Beverly, MA), HCV core (Abcam, Cambridge, MA), NS5A (BioDesign, Saco, ME), GRP78, GADD153/CHOP (Santa Cruz Biotechnology, Santa Cruz, CA), disulfide isomerase (PDI) (Stressgen Biotechnologies, Victoria, British Columbia, Canada), and beta-actin antibody (Sigma). Secondary antibodies were peroxidase-labeled anti-mouse, anti-rabbit antibody (GE Healthcare, Connecticut), donkey anti-goat IgG-horseradish peroxidase (HRP) antibody (Santa Cruz Biotechnology, Santa Cruz, CA), and Alexa 405-labeled goat anti-mouse and Alexa 568-labeled donkey anti-rabbit IgG antibodies (Invitrogen, Carlsbad, CA).

Cells and cell culture. Huh7 cells were maintained in Dulbecco's modified minimal essential medium (DMEM) (Sigma Chemical Co, St. Louis, MO) supplemented with 2 mmol/liter L-glutamine and 10% fetal bovine serum at 37°C under 5.0% CO_2.

Sequence analyses. Nucleotide sequences were read from both strands using BigDye Terminator cycle sequencing ready reaction kits (Applied Biosystems, Foster City, CA) and an automated DNA sequencer (ABI Prism 310 genetic analyzer; Applied Biosystems).

Establishment of mutant HCV clones. In order to introduce various mutations into the core region of JFH1, plasmid pJFH1full was digested with EcoRI and BsiWI, and then the DNA fragment encompassing nucleotides 1 to 456 was subcloned into the pGEM-T Easy vector (Promega, Madison, WI). The following mutations were introduced into the DNA fragment in the subcloning vector by site-directed mutagenesis (Quick-Change II site-directed mutagenesis kit; Stratagene): R70Q, R70H, L91M, and GKPG77-80KKKK. Finally, the EcoRI-BsiWI fragments were subcloned back into the parental plasmid, pJFH1full.

In vitro RNA synthesis and transfection. Full-length HCV expression plasmids were as follows: pJFH1full, which encodes the full-length HCV-JFH1 sequence (60), pR70Q, pR70H, pL91M, and p7780K. These plasmids were linearized at their 3′ ends and used as templates for HCV RNA synthesis using the RiboMax large-scale RNA production system (Promega, Madison, WI). After DNase I (RQ-1 RNase-free DNase; Promega) treatment, the transcribed HCV RNA was purified using Isogen reagent (Nippon Gene, Tokyo, Japan). For the RNA transfection, Huh7 cells were washed twice in phosphate-buffered saline (PBS), and 5×10^6 cells were suspended in Opti-MEM I (Invitrogen, Carlsbad, CA) containing 10 μg of HCV RNA, transferred into a 4-mm electroporation cuvette, and finally subjected to an electric pulse (1,050 μF and 270 V) using the Easy Jet system (EquiBio, Middlesex, United Kingdom). After electroporation, the cell suspension was left for 5 min at room temperature and then incubated under normal culture conditions in a 10-cm-diameter cell culture dish. Forty-eight hours after transfection, the levels of HCV replication and viral protein expression were detected by real-time PCR and Western blotting.

HCVcc infection analyses. Huh7 cells were plated on 12-well plates at a density of 1.2×10^4 cells per well. Supernatants from HCV RNA-transfected cells were inoculated onto each well at a titer of 8×10^5 copies/well (quantified by real-time reverse transcriptase PCR [RT-PCR]). Forty-eight hours after infection, various amounts of interferon were added, and the cells were harvested after 72 h of the interferon treatment (48).

RNA extraction, cDNA synthesis, and real-time RT-PCR analysis. For the detection of HCV RNA in culture supernatant, the supernatant was passed through a 0.45-μm filter (Millex-HA, Millipore, Bedford, MA) and stored at −80°C until use. Protocols and primers for the real-time RT-PCR analysis of HCV RNA have been described previously (48). For the detection of endogenous mRNAs, total cellular RNA was isolated using an RNeasy Mini kit (Qiagen, Valencia, CA). Two micrograms of total cellular RNA was used to generate cDNA from each sample using SuperScript II reverse transcriptase (Invitrogen, Carlsbad, CA). Expression of mRNA was quantified using the TaqMan universal PCR master mix (Applied Biosystems, Foster City, CA) and the ABI 7500 real-time PCR system (Applied Biosystems, Foster City, CA).

Luciferase assays. Luciferase activities were measured using a luminometer (Lumat LB9501; Promega) using the Dual-Luciferase reporter assay system (Promega). Assays were performed in triplicate.

Western blot analysis. Western blotting was carried out as described previously (24, 53, 63). Briefly, 10 mg of total cell lysate was separated using NuPAGE 4%–12% Bis-Tris gels (Invitrogen) and blotted onto a polyvinylidene fluoride (PVDF) Western blotting membrane (Roche). The membrane was incubated with the primary antibodies followed by a peroxidase-labeled anti-IgG antibody and visualized by chemiluminescence using the ECL Western blotting analysis system (Amersham Biosciences, Buckinghamshire, United Kingdom).

Immunohistochemistry. HCV-transfected Huh7 cells were cultured on 18-mm round micro cover glasses (Matsunami, Tokyo, Japan). For detection of HCV core, lipid droplet, and endoplasmic reticulum (ER), cells were fixed with cold acetone for 15 min. The cells were incubated with the primary antibodies for 1 h at 37°C. The fluorescent secondary antibodies were Alexa 405 goat anti-mouse and 568 donkey anti-rabbit IgG antibodies (Invitrogen, Carlsbad, CA). Lipid droplets (LDs) were visualized by using Bodipy 493/503 dye (Invitrogen). Cells were mounted with Vecta Shield mounting medium and 4′,6-diamidino-2-phenylindole (DAPI) (Vector Laboratories, Burlingame, CA) and visualized by using a confocal laser scanning microscope (FV10i; Olympus, Tokyo, Japan).

Calculation of 50% effective concentrations (EC_{50}). The EC_{50} was calculated as the concentration of IFN required for 50% reduction in HCV RNA expression. We used the probit regression analysis to obtain values.

Statistical analyses. Statistical analyses were performed by using Welch's *t* test. *P* values of less than 0.05 were considered statistically significant.

RESULTS

HCV core 70/91 mutants show resistance to IFN treatment. First, we investigated sensitivity to IFN treatment of the HCV core mutant R70Q, R70H, and L91M virus clones and compared them to the wild type. The wild type and core mutants were transfected into Huh7 cells, which were cultured in the presence of various concentrations of IFN-α for 48 h. RNA was extracted from the cells and culture supernatant, and the level of HCV RNA was quantified by real-time RT-PCR. Although the levels of supernatant HCV RNA did not differ between the wild type and core mutants (Fig. 1A), the levels of cellular HCV RNA showed that all three core mutants were significantly resistant to IFN compared to the wild type, with EC_{50}s of 5.0 IU/ml, 48 IU/ml, 32 IU/ml, and 47 IU/ml for the R70Q, R70H, L91M, and mutants and the wild type, respectively (Fig. 1B). To exclude the possible effects on interferon signaling by the input HCV RNA, we performed interferon sensitivity analyses by HCVcc infection. As shown in Fig. 1C, the interferon sensitivities of HCV core mutants and the wild type were consistent with the results of HCV RNA transfection. Similarly, according to Western blotting, the core mutants were more resistant to IFN treatment than the wild type (Fig. 1D).

Core mutants show decreased secretion of viral particles. To determine the mechanisms underlying the resistance to interferon, we compared baseline virus expression levels in cells and culture supernatants. The three core mutants, carrying R70Q, R70H, and L91M, expressed significantly higher levels of intracellular HCV RNA than the wild type, as well as the 7780K clone. (Fig. 2A). 7780K was a negative-control clone that lacked virus particle secretion (37). On the contrary, these core mutants released significantly smaller amounts of HCV RNA into the culture supernatant than the wild type, as well as the negative-control 7780K clone. (Fig. 2B). Consistent with the HCV RNA data, Western blotting showed that cellular HCV core protein levels were higher for the core amino acid 70/91 mutants than the wild type (Fig. 2C). These results suggested that the core 70/91 mutant clones were partially defective in the secretion of infectious virus particles.

Subcellular localization of wild-type and mutant core proteins and lipid droplets. It has been reported that HCV core protein localizes on the cellular LD membrane and may mediate encapsidation of viral genomic RNA and subsequent virus assembly (35, 36). Therefore, we visualized the subcellular localization of wild-type and mutant core proteins in rela-

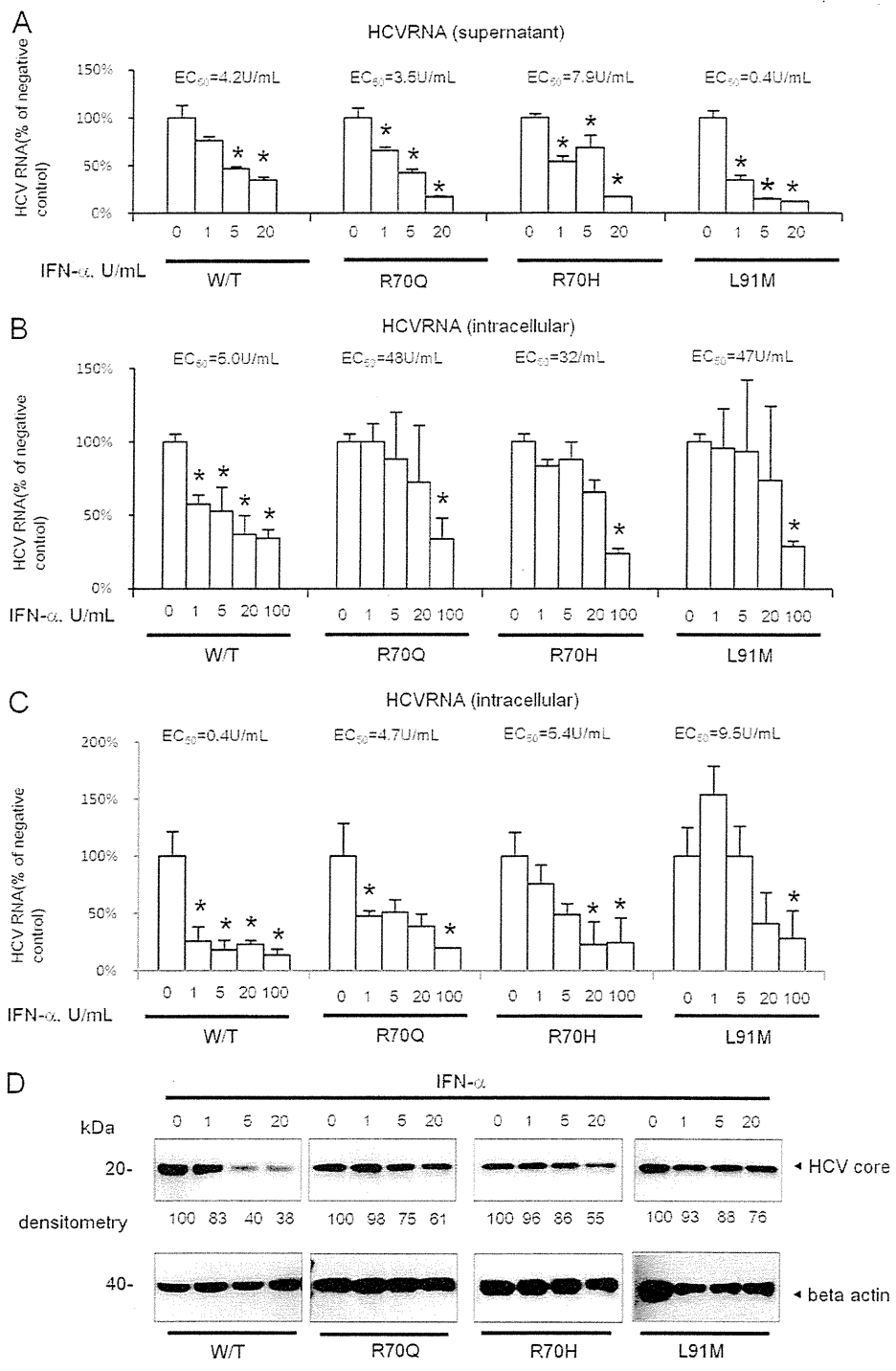

FIG. 1. Comparison of interferon sensitivity between HCV wild type and core mutant clones. The wild type and core mutants were transfected into Huh7 cells and cultured in the presence of IFN-α2b at concentrations ranging from 0 to 100 U/ml. (A) The culture supernatant of HCV-transfected Huh7 cells was collected 72 h after transfection, and the levels of HCV core antigen in the culture supernatant were measured. The values are displayed as percentages of those for the IFN-untreated control. The experiments were repeated three times, and representative results are shown. (B) Expression of intracellular HCV RNA. Cellular RNA was harvested at 72 h posttransfection. HCV RNA was quantified by real-time RT-PCR. The values are displayed as percentages of those for the IFN-untreated control. (C) Expression of intracellular HCV RNA. Cellular RNA was harvested at 72 h postinfection. HCV RNA was quantified by real-time RT-PCR. The values are displayed as percentages of those for the IFN-untreated control. In panels A through C, asterisks indicate *P* values of less than 0.05, compared to results for the interferon-negative control. (D) Western blotting was performed to assess intracellular suppression of HCV core protein. Ten micrograms of harvested cell lysates were subjected to Western blotting using anti-HCV core antibodies. Densitometry of core protein was performed, and results are shown as percentages of the results for an IFN-negative sample.

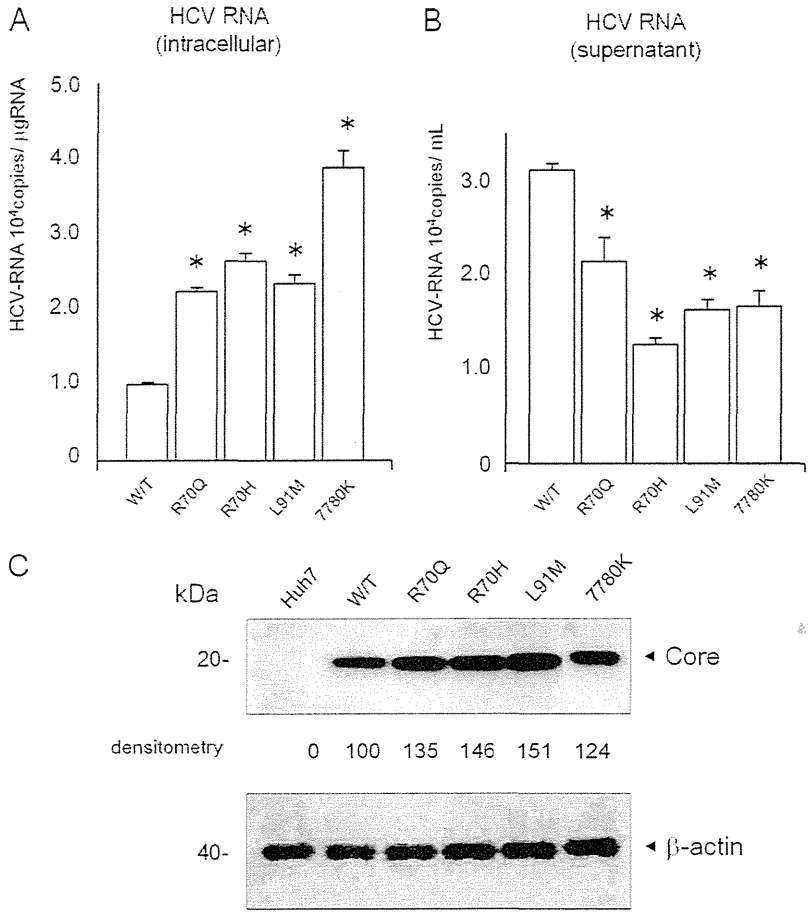

FIG. 2. Analysis of intracellular and supernatant HCV RNA levels in core 70/91 mutants. *In vitro*-transcribed mutant and wild-type RNAs were transfected into Huh7 cells. Three days after transfection, RNA was extracted from cells (A) or culture supernatant (B) and quantified by real-time RT-PCR. Asterisks indicate *P* values of less than 0.05 compared to results for the wild type. (C) Western blotting. Expression of core proteins in HCV-transfected cells. Total cellular protein was prepared from HCV RNA-transfected cells, and Western blotting was performed using anticore and anti-beta-actin antibodies. Densitometry was performed, and results are shown as percentages of that for an HCV-negative sample.

tion to that of LDs and the ER by indirect immunofluorescence and confocal microscopy. Consistent with previous reports, core proteins were colocalized with LDs but not with an ER-located protein, PDI, in the HCV-transfected cells (see the figure in the supplemental material). There were no obvious differences in colocalization of core and LDs or core and ER between the wild type and mutant core proteins.

Induction of interferon-stimulated genes following treatment of HCV-transfected cells with interferon. To investigate the mechanism of the relative IFN resistance of the core 70/91 mutants, as demonstrated in Fig. 1, we analyzed the cellular IFN signaling pathway. First, we assessed the expression and IFN-mediated induction of the mRNA transcripts of the IFN-stimulated genes (ISGs), encoding P56, double-stranded RNA-dependent protein kinase R (PKR), and 2′,5′-oligoadenylate synthetase (25AS), which mediate direct antiviral effects on HCV expression (24, 25). Cellular expression of PKR, P56, and 25AS was substantially increased in HCV-transfected cells, as well as naive cells, following IFN treatment. However, the levels of induction were significantly lower in the three HCV core mutant-transfected cells than in wild-type-transfected cells (Fig. 3A, B, and C). We next detected IFN-induced phosphorylation of STAT1 and STAT2 in the mutant and wild-type HCV-expressing cells. Our previous experiments showed that the levels of phosphorylated STAT1 and STAT2 (pSTAT1 and pSTAT2, respectively) increased within minutes of the addition of IFN and decreased subsequently at 8 h (25). Therefore, we detected pSTAT1 and pSTAT2 levels before and at 15 min after the addition of IFN. As shown in Fig. 3D and E, levels of pSTAT1 and pSTAT2 were lower in core mutant-transfected and -infected cells after IFN treatment than in wild-type-transfected cells and naive cells. These findings indicate that the differences in sensitivity to interferon of core mutant clones and the wild type were associated with attenuation of the cellular IFN signaling pathway.

SOCS3 is upregulated in core mutant clones-transfected, IFN-resistant cells. We examined next the effects of HCV replication on the expression of SOCS1 and SOCS3, proteins that suppress IFN receptor-mediated signaling (50, 58). There was no significant difference in expression levels of SOCS1

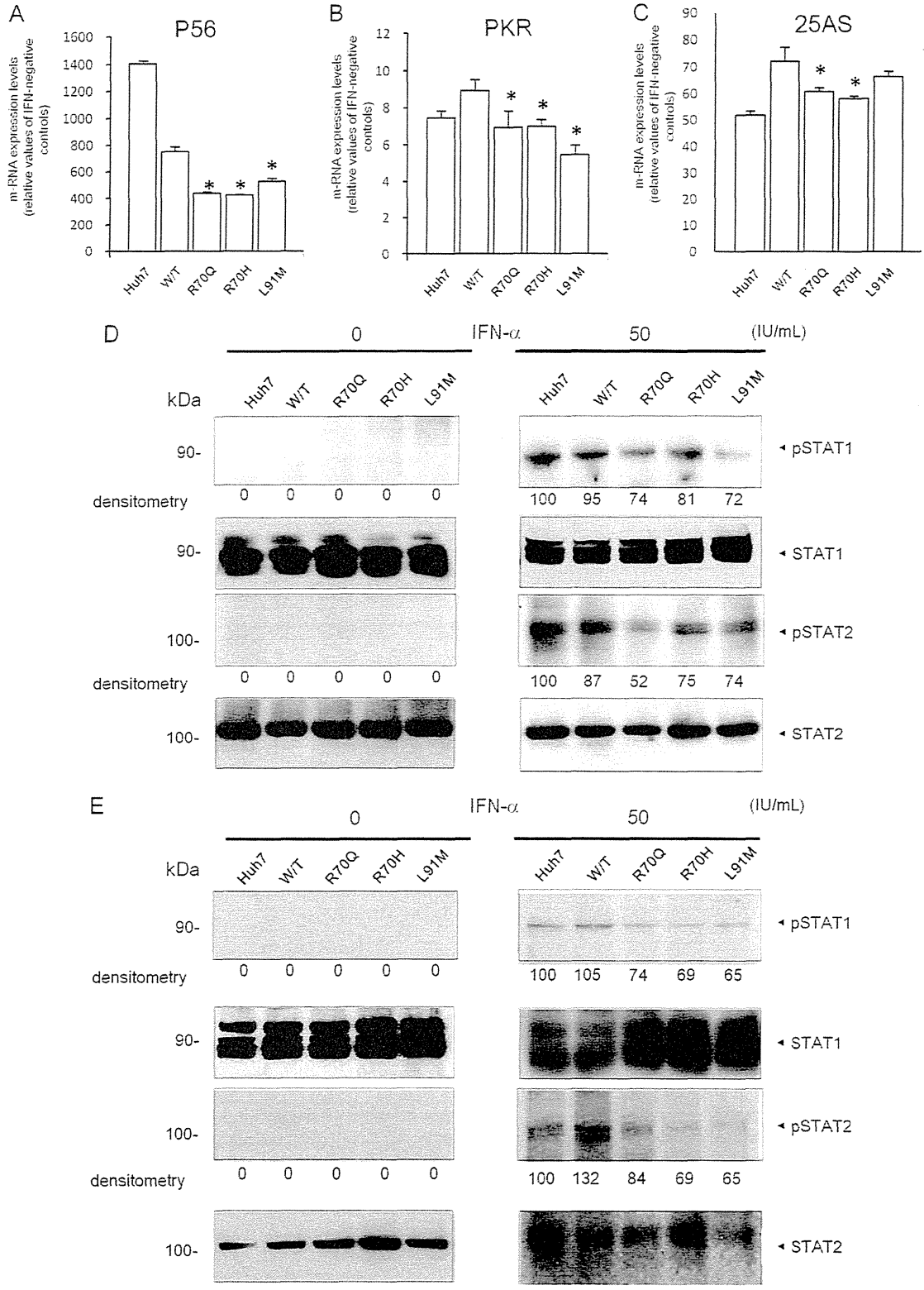

FIG. 3. Interferon-induced expressional induction of the ISGs, P56, PKR, and 25AS in Huh7 cells transfected or infected with wild-type and core mutant JFH1 clones. Two days posttransfection, cells were treated with 50 IU/ml of IFN-α. After 8 h, total cellular RNA was extracted and mRNAs of P56 (A), PKR (B), or 25AS (C) were quantified by real-time RT-PCR analyses. The values are displayed as ratios of IFN-untreated control values. Experiments were repeated three times, and representative results are shown. Asterisks indicate *P* values of less than 0.05 compared to results for the wild type. (D) Western blotting. Expression of total and phosphorylated STAT1 and STAT2 proteins in cells transfected with the wild type and core mutant HCV clones. (E) Western blotting. Expression of total and phosphorylated STAT1 and STAT2 proteins in cells infected with the wild type and core mutant HCV clones. Densitometries for pSTAT1 and pSTAT2 were performed, and results are shown as percentage of results for HCV-negative samples.

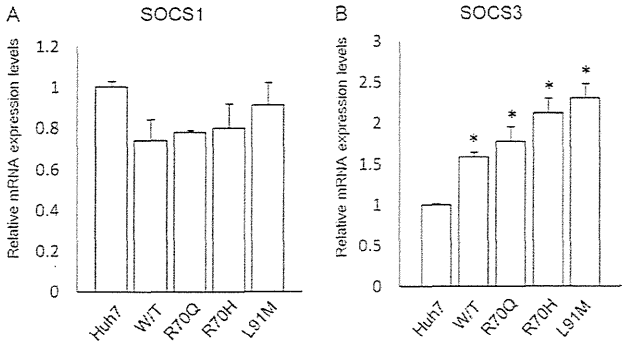

FIG. 4. Effects of core mutant HCV on SOCS1 and SOCS3 expression in Huh7 cells. Expression levels of SOCS1 (A) or SOCS3 (B) in Huh7 cells transfected with the wild type or the core mutant JFH1. Three days posttransfection, total cellular RNA was isolated and the mRNA was quantified by real-time RT-PCR analyses. The experiments were repeated three times, and representative results are shown. The values are displayed as values relative to beta-actin levels. Each experiment was repeated three times, and the representative results are shown. Asterisks indicate *P* values of less than 0.05 compared to results for the wild type.

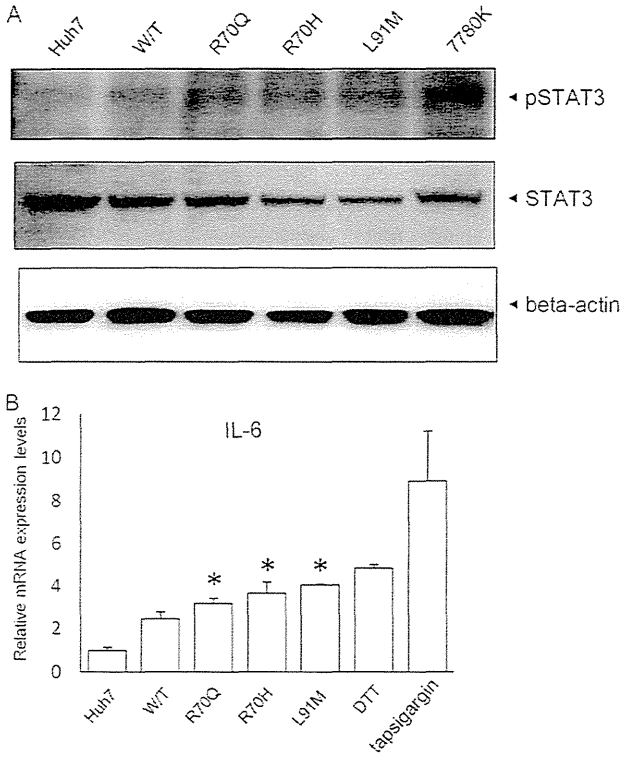

FIG. 5. Expression of phosphorylated STAT3 and IL-6 in cells transfected with the wild type and core mutant HCV-JFH1 clones. (A) Western blotting. Expression of total and phosphorylated STAT3 and beta-actin proteins in cells transfected with the wild type or core mutant HCV clones. (B) Two days posttransfection, total cellular RNA was extracted and mRNAs of IL-6 were quantified by real-time RT-PCR analyses. The values are displayed as the ratio of values of the HCV-untreated control. Asterisks indicate *P* values of less than 0.05 compared to results for the wild type.

mRNA between cells transfected with the wild type and the core mutant clones. In contrast, the SOCS3 mRNA expression level was significantly higher in core mutant-transfected cells than in wild-type-transfected cells (Fig. 4A and B). It is known that SOCS3 is induced principally by phosphorylated STAT3 (pSTAT3) (18) and that interleukin-6 (IL-6) is a strong inducer of pSTAT3 via receptor-mediated Janus kinase activation in the liver (41, 51). On that basis, we investigated whether overexpression of SOCS3 is associated with increased pSTAT3 and with overproduction of IL-6. The pSTAT3 level was significantly higher in core mutant-transfected cells than in JFH1-transfected cells and naive Huh7 cells (Fig. 5A). Moreover, cellular IL-6 mRNA expression was significantly higher in core mutant-transfected cells than in wild-type-transfected cells (Fig. 5B). These findings suggested that upregulation of cellular SOCS3 is associated with the resistance to IFN of the core 70/91 mutant HCV clones and that this effect is mediated partly by overproduction of IL-6.

UPRs are enhanced in core mutant-transfected cells. We have reported that HCV causes direct cytopathic effects on host cells and that these effects are mediated by HCV-induced unfolded protein responses (UPRs) (48). Therefore, we detected the expression of UPR-related proteins, GRP78 and CHOP, in cells expressing wild-type HCV and the core 70/91 mutants. As shown in Fig. 6, HCV-transfected cells showed higher expression levels of GRP78 and CHOP than untransfected cells. Furthermore, cells transfected with HCV core 70/91 mutant clones expressed larger amounts of GRP78 and CHOP than the wild-type-transfected cells. Because IL-6 is principally expressed following UPR induction (Fig. 5B), these data indicate that HCV-induced UPR may be involved in the IFN resistance of core mutant clones.

DISCUSSION

In this study, we used a virus cell culture system to investigate the characteristics of R70Q, R70H, and L91M HCV core mutant viruses, which were clinically resistant to peg-IFN-plus-RBV treatment, and found that these core mutant clones showed resistance to IFN *in vitro*, consistent with the clinical findings (Fig. 1). These differences in the IFN sensitivity of the core mutant clones led us conduct a series of experiments to investigate the molecular mechanisms of IFN-related response pathways. We found that IFN-α receptor-mediated signaling was attenuated in wild-type HCV-infected and core mutant-infected cells compared to that in uninfected cells and that the suppression of IFN signaling was more potent for core mutant clones than for the wild type. The differences in the interferon-mediated antiviral effects were demonstrated further by the difference in the induction rates of IFN-inducible P56, PKR, and 25AS mRNAs (Fig. 3A, B, and C) and IFN-induced phosphorylation of STAT1 and STAT2 (Fig. 3D and E). Furthermore, the expression levels of an interferon signal attenuator, SOCS3, were significantly higher in core mutant-transfected cells than in wild-type-transfected cells. Moreover, cellular expression of IL-6, which induces SOCS3 expression through phosphorylation of STAT3 (18, 41), was significantly higher in the core mutant-transfected cells than in wild-type-transfected cells (Fig. 5A). Taking all these things together, it is suggested strongly that the IFN resistance of core mutant clones is due to

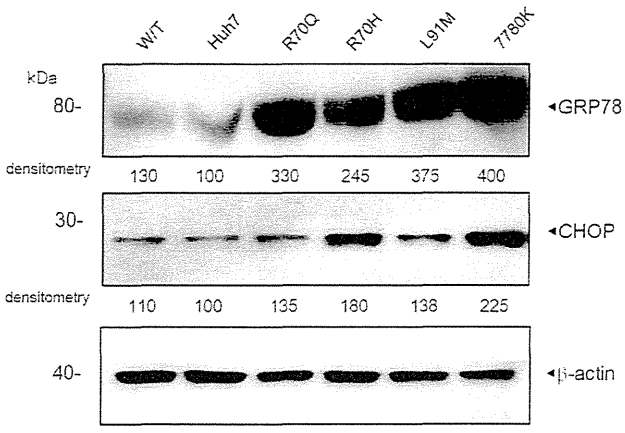

FIG. 6. Expression of GRP78 and CHOP UPR genes in cells transfected with the wild type and core mutant HCV-JFH1 clones. Western blotting was performed to assess UPR following transfection with HCV core mutants. Ten micrograms of harvested cell lysates were subjected to Western blotting using anti-GRP78 and anti-CHOP antibodies. Densitometries for GRP78 and CHOP were performed, and results are shown as percentages of results for uninfected cells.

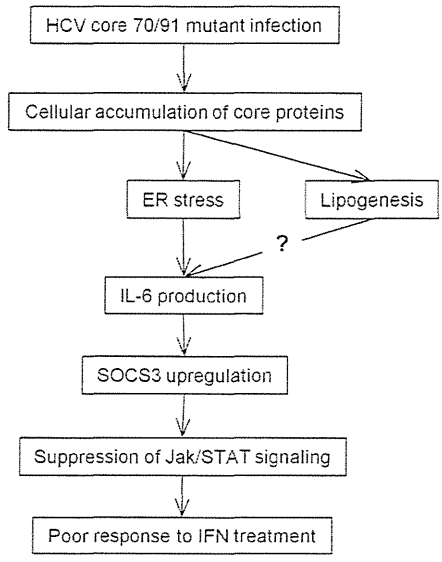

FIG. 7. Schematic diagram of signaling pathway involved in HCV core mutant infection and IFN resistance.

SOCS3-mediated attenuation of IFN responses and that, more importantly, upregulation of cellular IL-6 is attributable to emergence of IFN resistance (Fig. 7).

Miyanari et al. demonstrated that core protein, which is localized in LD-associated membrane, recruits HCV nonstructural (NS) proteins and replication complexes to LD and that this recruitment is critical for producing infectious viruses (35). Furthermore, Masaki et al. reported that the NS5A protein interacts with core at its C-terminal serine cluster and this NS5A-core interaction is crucial for the production of virus particle (32). In this study, there was no difference between the core mutants and the wild-type virus in terms of the pattern of colocalization of core protein with LDs and also the ER membrane (see the figure in the supplemental material). These results suggest that the core amino acid substitutions at positions 70 and 91 do not alter the characteristics of the core protein in terms of subcellular localization. Murray et al. conducted a comprehensive alanine substitution scan of the core protein to search for domains that are essential for virion production. They showed that substitutions of amino acids 70 and 91 spared but slightly decreased the capacity for virus particle production (37), which is consistent with our present results. Those mutations may cause accumulation of virus and core protein in the LDs and ER membrane and may elicit UPRs and IFN resistance.

Type I IFNs and their responsive ISGs are the principal mediators of host defense against virus infections, including HCV (10, 26, 44). Upon binding of IFNs to their receptors, IFNAR1 and IFNAR2, Janus kinases (Jak)1 and 2 phosphorylate STAT1 and STAT2 to form ISGF-3, which translocates to the nucleus and activates transcription of ISGs (46, 54, 55). Members of the SOCS family are potent inhibitors of type I and type III IFN-induced activation of the Jak-STAT pathway and subsequent expression of ISGs (58). HCV, on the other hand, counteracts such IFN-mediated antiviral pathways through its interaction with various steps of IFN signaling. The HCV NS5A and E2 proteins interfere with the action of IFN by inhibiting the activity of PKR (20, 56). NS5A also induces expression of IL-8 and attenuates expression of ISGs (40).

HCV core protein has been reported to interfere with the antiviral actions of IFN. Core protein binds the STAT1-SH domain (29) and destabilizes STAT1 (28) to block IFN signaling. Blindenbacher et al. (8) showed that STAT signaling was strongly inhibited in the hepatocytes of HCV core transgenic mice. Bode et al. showed that HCV core protein induced SOCS3 expression and inhibited tyrosine phosphorylation of STAT1 in HepG2 cells (9). In this study, we used full-length HCV cell culture and found that SOCS3 expression is upregulated at different rates, depending on the genetic sequences of HCV strains, and that these differences in SOCS3 expression are associated with sensitivity to IFN. These results indicate that the IFN resistance of HCV-infected cells is mediated by overexpression of SOCS3, which may be upregulated by HCV proteins, as previously reported (9, 27). Only one amino acid difference, R70Q, R70H, or L91M, might have affected cellular responses to interferon.

IL-6 is the principal activator of STAT3 in hepatocytes (18, 41). It has been reported that plasma IL-6 levels are elevated in CHC patients (30). Basu et al. have conducted DNA microarray analyses in HCV core-expressing cells and demonstrated that genes including those encoding IL-6 and STAT3 were upregulated by core protein (7). Consistent with these findings, we found that cellular IL-6 expression levels were elevated in HCV-transfected cells in the order (from lowest to highest levels) untransfected, wild type, and then core mutants, which correlated well with SOCS3 expression (Fig. 4B) and with cellular responses to IFN (Fig. 1B and C). The inducers of IL-6 remain to be clarified. IL-6 is secreted in response to cellular steatosis and insulin resistance (45). Hepatic steatosis is found in 70% of CHC patients (57) and those with obesity; steatosis or insulin resistance is refractory to IFN treatment (43). Such patients show higher levels of hepatic SOCS3 ex-

pression than those without obesity or insulin resistance (34, 61). We reported previously that a series of genes involved in fatty acid and cholesterol synthesis are upregulated in HCV replicon-expressing and HCV-JFH1-infected cells and increased cellular LDs (39). Such lipogenic cellular processes may be the cause of the upregulated expression of IL-6. Alternatively, UPRs may produce IL-6. Chen et al. have reported that UPRs are coupled with TNF-α and IL-6 production in human macrophages (11). In this study, transfection of Huh7 cells by HCV induced the expression of UPR genes, and their expression levels were significantly higher in mutant core protein-transfected cells than in wild type-transfected cells (Fig. 6).

The differences in ISG expression levels between the HCV wild type and core mutants were significant but small (Fig. 3A, B, and C). As shown in Fig. 3D, and E and 4B, the interclone differences in pSTAT and SOCS3 were significant but relatively small, which may explain the small differences in ISG levels. Similarly, the clinical difference in interferon treatment outcomes between core 70/91 mutants and wild types are significant but are around the sustained viral clearance rates of 32.4% versus 53.5% in core 70 or 91 mutants and wild types, respectively (19), which might be consistent with our present results.

In clinical settings, IFN resistance of the core amino acid 70/91 mutants has been reported for genotype 1b strains (5). At present, there is no report that these mutations are associated with IFN treatment responses to other genotypes, including genotype 2a, which we used in this study. Because HCV strains other than genotypes 1 and 4 are generally sensitive to IFN, the core 70/91 mutations might not affect final treatment outcomes. We have conducted preliminary experiments using genotype 1b infectious clones with low levels of replication and found that these mutations did not significantly affect sensitivity to IFN in culture. It may be necessary to investigate IFN sensitivity when efficient cell culture systems have been developed for HCV genotype 1.

In addition to the poor virological responses of HCV core amino acid 70/91 mutants to peg-IFN-plus-RBV treatment (4, 6, 12), patients infected with the core mutants showed increased incidence of hepatocellular malignancies (2, 15, 49). It has been reported that the HCV core R70 but not L91 mutant frequently causes steatosis and increased hepatic oxidative stress (52). It is possible that core 70/91 mutations not only induce IFN resistance but also may cause other pathophysiological conditions, such as carcinogenesis and disorders of lipid metabolism.

In conclusion, our study demonstrates that the IFN resistance of HCV core mutants may be, for the most part, determined by cellular expression levels of SOCS3 and IL-6. Therapeutic targeting of IL-6 potentially may be a key to targeting IFN resistance and improving antiviral chemotherapeutics against HCV.

ACKNOWLEDGMENTS

We thank Takaji Wakita for providing pJFH1full.

This study was supported by grants from the Ministry of Education, Culture, Sports, Science and Technology—Japan, the Japan Society for the Promotion of Science, Ministry of Health, Labor and Welfare—Japan, Japan Health Sciences Foundation, and National Institute of Biomedical Innovation.

REFERENCES

1. **Akuta, N., et al.** 2010. Amino acid substitution in HCV core region and genetic variation near IL28B gene predict viral response to telaprevir with peginterferon and ribavirin. Hepatology **52:**421–429.
2. **Akuta, N., et al.** 2007. Amino acid substitutions in the hepatitis C virus core region are the important predictor of hepatocarcinogenesis. Hepatology **46:**1357–1364.
3. **Akuta, N., et al.** 2008. Efficacy of low-dose intermittent interferon-alpha monotherapy in patients infected with hepatitis C virus genotype 1b who were predicted or failed to respond to pegylated interferon plus ribavirin combination therapy. J. Med. Virol. **80:**1363–1369.
4. **Akuta, N., et al.** 2007. Predictive factors of early and sustained responses to peginterferon plus ribavirin combination therapy in Japanese patients infected with hepatitis C virus genotype 1b: amino acid substitutions in the core region and low-density lipoprotein cholesterol levels. J. Hepatol. **46:**403–410.
5. **Akuta, N., et al.** 2005. Virological and biochemical relapse after discontinuation of lamivudine monotherapy for chronic hepatitis B in Japan: comparison with breakthrough hepatitis during long-term treatment. Intervirology **48:**174–182.
6. **Akuta, N., et al.** 2005. Association of amino acid substitution pattern in core protein of hepatitis C virus genotype 1b high viral load and non-virological response to interferon-ribavirin combination therapy. Intervirology **48:**372–380.
7. **Basu, A., et al.** 2006. Microarray analyses and molecular profiling of Stat3 signaling pathway induced by hepatitis C virus core protein in human hepatocytes. Virology **349:**347–358.
8. **Blindenbacher, A., et al.** 2003. Expression of hepatitis c virus proteins inhibits interferon alpha signaling in the liver of transgenic mice. Gastroenterology **124:**1465–1475.
9. **Bode, J. G., et al.** 2003. IFN-alpha antagonistic activity of HCV core protein involves induction of suppressor of cytokine signaling-3. FASEB J. **17:**488–490.
10. **Chang, K. C., E. Hansen, L. Foroni, J. Lida, and G. Goldspink.** 1991. Molecular and functional analysis of the virus- and interferon-inducible human MxA promoter. Arch. Virol. **117:**1–15.
11. **Chen, L., et al.** 2009. HIV protease inhibitor lopinavir-induced TNF-alpha and IL-6 expression is coupled to the unfolded protein response and ERK signaling pathways in macrophages. Biochem. Pharmacol. **78:**70–77.
12. **Donlin, M. J., et al.** 2007. Pretreatment sequence diversity differences in the full-length hepatitis C virus open reading frame correlate with early response to therapy. J. Virol. **81:**8211–8224.
13. **Enomoto, N., et al.** 1996. Mutations in the nonstructural protein 5A gene and response to interferon in patients with chronic hepatitis C virus 1b infection. N. Engl. J. Med. **334:**77–81.
14. **Farci, P., et al.** 2002. Early changes in hepatitis C viral quasispecies during interferon therapy predict the therapeutic outcome. Proc. Natl. Acad. Sci. U. S. A. **99:**3081–3086.
15. **Fishman, S. L., et al.** 2009. Mutations in the hepatitis C virus core gene are associated with advanced liver disease and hepatocellular carcinoma. Clin. Cancer Res. **15:**3205–3213.
16. **Fried, M. W., et al.** 2002. Peginterferon alfa-2a plus ribavirin for chronic hepatitis C virus infection. N. Engl. J. Med. **347:**975–982.
17. **George, S. L., et al.** 2009. Clinical, virologic, histologic, and biochemical outcomes after successful HCV therapy: a 5-year follow-up of 150 patients. Hepatology **49:**729–738.
18. **Hanada, T., I. Kinjyo, K. Inagaki-Ohara, and A. Yoshimura.** 2003. Negative regulation of cytokine signaling by CIS/SOCS family proteins and their roles in inflammatory diseases. Rev. Physiol. Biochem. Pharmacol. **149:**72–86.
19. **Hayes, C. N., et al.** 2010. HCV substitutions and IL28B polymorphisms on outcome of peg-interferon plus ribavirin combination therapy. Gut **60:**261–267.
20. **He, Y., and M. G. Katze.** 2002. To interfere and to anti-interfere: the interplay between hepatitis C virus and interferon. Viral Immunol. **15:**95–119.
21. **Heathcote, E. J., et al.** 2000. Peginterferon alfa-2a in patients with chronic hepatitis C and cirrhosis. N. Engl. J. Med. **343:**1673–1680.
22. **Honda, T., et al.** 2007. Efficacy of ribavirin plus interferon-alpha in patients aged >or=60 years with chronic hepatitis C. J. Gastroenterol. Hepatol. **22:**989–995.
23. **Hung, C. H., et al.** 2008. Association of amino acid variations in the NS5A and E2-PePHD region of hepatitis C virus 1b with hepatocellular carcinoma. J. Viral Hepat. **15:**58–65.
24. **Itsui, Y., et al.** 2009. Antiviral effects of the interferon-induced protein guanylate binding protein 1 and its interaction with the hepatitis C virus NS5B protein. Hepatology **50:**1727–1737.
25. **Itsui, Y., et al.** 2006. Expressional screening of interferon-stimulated genes for antiviral activity against hepatitis C virus replication. J. Viral Hepat. **13:**690–700.
26. **Kalvakolanu, D. V.** 2003. Alternate interferon signaling pathways. Pharmacol. Ther. **100:**1–29.

27. **Kawaguchi, T., et al.** 2004. Hepatitis C virus down-regulates insulin receptor substrates 1 and 2 through up-regulation of suppressor of cytokine signaling 3. Am. J. Pathol. **165:**1499–1508.
28. **Lin, W., et al.** 2005. Hepatitis C virus expression suppresses interferon signaling by degrading STAT1. Gastroenterology **128:**1034–1041.
29. **Lin, W., et al.** 2006. Hepatitis C virus core protein blocks interferon signaling by interaction with the STAT1 SH2 domain. J. Virol. **80:**9226–9235.
30. **Malaguarnera, M., et al.** 1997. Elevation of interleukin 6 levels in patients with chronic hepatitis due to hepatitis C virus. J. Gastroenterol. **32:**211–215.
31. **Manns, M. P., et al.** 2001. Peginterferon alfa-2b plus ribavirin compared with interferon alfa-2b plus ribavirin for initial treatment of chronic hepatitis C: a randomised trial. Lancet **358:**958–965.
32. **Masaki, T., et al.** 2008. Interaction of hepatitis C virus nonstructural protein 5A with core protein is critical for the production of infectious virus particles. J. Virol. **82:**7964–7976.
33. **Massard, J., et al.** 2006. Natural history and predictors of disease severity in chronic hepatitis C. J. Hepatol. **44:**S19–S24.
34. **Miyaaki, H., et al.** 2009. Predictive value of suppressor of cytokine signal 3 (SOCS3) in the outcome of interferon therapy in chronic hepatitis C. Hepatol. Res. **39:**850–855.
35. **Miyanari, Y., et al.** 2007. The lipid droplet is an important organelle for hepatitis C virus production. Nat. Cell Biol. **9:**1089–1097.
36. **Moradpour, D., C. Englert, T. Wakita, and J. R. Wands.** 1996. Characterization of cell lines allowing tightly regulated expression of hepatitis C virus core protein. Virology **222:**51–63.
37. **Murray, C. L., C. T. Jones, J. Tassello, and C. M. Rice.** 2007. Alanine scanning of the hepatitis C virus core protein reveals numerous residues essential for production of infectious virus. J. Virol. **81:**10220–10231.
38. **Nakagawa, M., et al.** 2010. Mutations in the interferon sensitivity determining region and virological response to combination therapy with pegylated-interferon alpha 2b plus ribavirin in patients with chronic hepatitis C-1b infection. J. Gastroenterol. **45:**656–665.
39. **Nishimura-Sakurai, Y., et al.** 2010. Comparison of HCV-associated gene expression and cell signaling pathways in cells with or without HCV replicon and in replicon-cured cells. J. Gastroenterol. **45:**523–536.
40. **Polyak, S. J., K. S. Khabar, M. Rezeiq, and D. R. Gretch.** 2001. Elevated levels of interleukin-8 in serum are associated with hepatitis C virus infection and resistance to interferon therapy. J. Virol. **75:**6209–6211.
41. **Ramadori, G., and B. Christ.** 1999. Cytokines and the hepatic acute-phase response. Semin. Liver Dis. **19:**141–155.
42. **Roffi, L., et al.** 2008. Pegylated interferon-alpha2b plus ribavirin: an efficacious and well-tolerated treatment regimen for patients with hepatitis C virus related histologically proven cirrhosis. Antivir. Ther. **13:**663–673.
43. **Romero-Gomez, M., et al.** 2005. Insulin resistance impairs sustained response rate to peginterferon plus ribavirin in chronic hepatitis C patients. Gastroenterology **128:**636–641.
44. **Ronni, T., et al.** 1998. The proximal interferon-stimulated response elements are essential for interferon responsiveness: a promoter analysis of the antiviral MxA gene. J. Interferon Cytokine Res. **18:**773–781.
45. **Sabio, G., et al.** 2008. A stress signaling pathway in adipose tissue regulates hepatic insulin resistance. Science **322:**1539–1543.
46. **Samuel, C.** 2001. Antiviral actions of interferons. Clin. Microbiol. Rev. **14:**778–809.
47. **Santantonio, T., et al.** 2003. Natural course of acute hepatitis C: a long-term prospective study. Dig. Liver Dis. **35:**104–113.
48. **Sekine-Osajima, Y., et al.** 2008. Development of plaque assays for hepatitis C virus-JFH1 strain and isolation of mutants with enhanced cytopathogenicity and replication capacity. Virology **371:**71–85.
49. **Sobesky, R., et al.** 2007. Distinct hepatitis C virus core and F protein quasispecies in tumoral and nontumoral hepatocytes isolated via microdissection. Hepatology **46:**1704–1712.
50. **Song, M. M., and K. Shuai.** 1998. The suppressor of cytokine signaling (SOCS) 1 and SOCS3 but not SOCS2 proteins inhibit interferon-mediated antiviral and antiproliferative activities. J. Biol. Chem. **273:**35056–35062.
51. **Suda, G., et al.** 2010. IL-6-mediated intersubgenotypic variation of interferon sensitivity in hepatitis C virus genotype 2a/2b chimeric clones. Virology **407:**80–90.
52. **Tachi, Y., et al.** 2010. Impact of amino acid substitutions in the hepatitis C virus genotype 1b core region on liver steatosis and hepatic oxidative stress in patients with chronic hepatitis C. Liver Int. **30:**554–559.
53. **Tanabe, Y., et al.** 2004. Synergistic inhibition of intracellular hepatitis C virus replication by combination of ribavirin and interferon-alpha. J. Infect. Dis. **189:**1129–1139.
54. **Taniguchi, T., K. Ogasawara, A. Takaoka, and N. Tanaka.** 2001. IRF family of transcription factors as regulators of host defense. Annu. Rev. Immunol. **19:**623–655.
55. **Taniguchi, T., and A. Takaoka.** 2002. The interferon-alpha/beta system in antiviral responses: a multimodal machinery of gene regulation by the IRF family of transcription factors. Curr. Opin. Immunol. **14:**111–116.
56. **Taylor, D. R., S. T. Shi, P. R. Romano, G. N. Barber, and M. M. Lai.** 1999. Inhibition of the interferon-inducible protein kinase PKR by HCV E2 protein. Science **285:**107–110.
57. **Vidali, M., et al.** 2008. Interplay between oxidative stress and hepatic steatosis in the progression of chronic hepatitis C. J. Hepatol. **48:**399–406.
58. **Vlotides, G., et al.** 2004. SOCS-1 and SOCS-3 inhibit IFN-alpha-induced expression of the antiviral proteins 2,5-OAS and MxA. Biochem. Biophys. Res. Commun. **320:**1007–1014.
59. **von Wagner, M., et al.** 2003. Dynamics of hepatitis C virus quasispecies turnover during interferon-alpha treatment. J. Viral Hepat. **10:**413–422.
60. **Wakita, T., et al.** 2005. Production of infectious hepatitis C virus in tissue culture from a cloned viral genome. Nat. Med. **11:**791–796.
61. **Walsh, M. J., et al.** 2006. Non-response to antiviral therapy is associated with obesity and increased hepatic expression of suppressor of cytokine signalling 3 (SOCS-3) in patients with chronic hepatitis C, viral genotype 1. Gut **55:**529–535.
62. **Wiese, M., et al.** 2005. Outcome in a hepatitis C (genotype 1b) single source outbreak in Germany—a 25-year multicenter study. J. Hepatol. **43:**590–598.
63. **Yokota, T., et al.** 2003. Inhibition of intracellular hepatitis C virus replication by synthetic and vector-derived small interfering RNAs. EMBO Rep. **4:**602–608.
64. **Yoshida, H., et al.** 2004. Benefit of interferon therapy in hepatocellular carcinoma prevention for individual patients with chronic hepatitis C. Gut **53:**425–430.
65. **Zhong, J., et al.** 2005. Robust hepatitis C virus infection in vitro. Proc. Natl. Acad. Sci. U. S. A. **102:**9294–9299.

Research Article

EASL EUROPEAN ASSOCIATION FOR THE STUDY OF THE LIVER | JOURNAL OF HEPATOLOGY

Pre-treatment prediction of response to pegylated-interferon plus ribavirin for chronic hepatitis C using genetic polymorphism in *IL28B* and viral factors

Masayuki Kurosaki[1], Yasuhito Tanaka[2], Nao Nishida[3], Naoya Sakamoto[4], Nobuyuki Enomoto[5], Masao Honda[6], Masaya Sugiyama[2], Kentaro Matsuura[2], Fuminaka Sugauchi[2], Yasuhiro Asahina[1], Mina Nakagawa[4], Mamoru Watanabe[4], Minoru Sakamoto[5], Shinya Maekawa[5], Akito Sakai[6], Shuichi Kaneko[6], Kiyoaki Ito[7], Naohiko Masaki[7], Katsushi Tokunaga[3], Namiki Izumi[1,*], Masashi Mizokami[2,7]

[1]*Division of Gastroenterology and Hepatology, Musashino Red Cross Hospital, Tokyo, Japan;* [2]*Department of Virology, Liver Unit, Nagoya City University, Graduate School of Medical Sciences, Nagoya, Japan;* [3]*Department of Human Genetics, Graduate School of Medicine, University of Tokyo, Tokyo, Japan;* [4]*Department of Gastroenterology and Hepatology, Tokyo Medical and Dental University, Tokyo, Japan;* [5]*First Department of Internal Medicine, University of Yamanashi, Yamanashi, Japan;* [6]*Department of Gastroenterology, Kanazawa University, Graduate School of Medicine, Kanazawa, Japan;* [7]*Research Center for Hepatitis and Immunology, International Medical Center of Japan, Konodai Hospital, Ichikawa, Japan*

Background & Aims: Pegylated interferon and ribavirin (PEG-IFN/RBV) therapy for chronic hepatitis C virus (HCV) genotype 1 infection is effective in 50% of patients. Recent studies revealed an association between the *IL28B* genotype and treatment response. We aimed to develop a model for the pre-treatment prediction of response using host and viral factors.

Methods: Data were collected from 496 patients with HCV genotype 1 treated with PEG-IFN/RBV at five hospitals and universities in Japan. *IL28B* genotype and mutations in the core and IFN sensitivity determining region (ISDR) of HCV were analyzed to predict response to therapy. The decision model was generated by data mining analysis.

Results: The *IL28B* polymorphism correlated with early virological response and predicted null virological response (NVR) (odds ratio = 20.83, p <0.0001) and sustained virological response (SVR) (odds ratio = 7.41, p <0.0001) independent of other covariates. Mutations in the ISDR predicted relapse and SVR independent of *IL28B*. The decision model revealed that patients with the minor *IL28B* allele and low platelet counts had the highest NVR (84%) and lowest SVR (7%), whereas those with the major *IL28B* allele and mutations in the ISDR or high platelet counts had the lowest NVR (0–17%) and highest SVR (61–90%). The model had high reproducibility and predicted SVR with 78% specificity and 70% sensitivity.

Conclusions: The *IL28B* polymorphism and mutations in the ISDR of HCV were significant pre-treatment predictors of response to PEG-IFN/RBV. The decision model, including these host and viral factors may support selection of optimum treatment strategy for individual patients.

Keywords: *IL28B*; ISDR; Peg-interferon; Ribavirin; Data mining; Decision tree.
Received 14 March 2010; received in revised form 22 June 2010; accepted 7 July 2010; available online 19 September 2010

* Corresponding author. Address: Division of Gastroenterology and Hepatology, Musashino Red Cross Hospital, 1-26-1 Kyonan-cho, Musashino-shi, Tokyo 180-8610, Japan. Tel.: +81 422 32 3111; fax: +81 422 32 9551.
E-mail address: nizumi@musashino.jrc.or.jp (N. Izumi).

Introduction

Hepatitis C virus (HCV) infection is the leading cause of cirrhosis and hepatocellular carcinoma worldwide [1]. The successful eradication of HCV, defined as a sustained virological response (SVR), is associated with a reduced risk of developing hepatocellular carcinoma. Currently, pegylated interferon (PEG-IFN) plus ribavirin (RBV) is the most effective standard of care for chronic hepatitis C but the rate of SVR is around 50% in patients with HCV genotype 1 [2,3], the most common genotype in Japan, Europe, the United States, and many other countries. Moreover, 20–30% of patients with HCV genotype 1 have a null virological response (NVR) to PEG-IFN/RBV therapy [4]. The most reliable method for predicting the response is to monitor the early decline of serum HCV-RNA levels during treatment [5] but there is no established method for prediction before treatment. Because PEG-IFN/RBV therapy is costly and often accompanied by adverse effects such as flu-like symptoms, depression and hematological abnormalities, pre-treatment predictions of those patients who are unlikely to benefit from this regimen enables ineffective treatment to be avoided.

Recently, it has been reported through a genome-wide association study (GWAS) of patients with genotype 1 HCV that single nucleotide polymorphisms (SNPs) located near the *IL28B* gene are strongly associated with a response to PEG-IFN/RBV therapy in

Research Article

Table 1. Baseline characteristics of all patients, and patients assigned to the model building or validation groups.

	All patients n = 496	Model group n = 331	Validation group n = 165
Gender: male	250 (50%)	170 (51%)	80 (48%)
Age (years)	57.1 ± 9.9	56.8 ± 9.7	57.5 ± 10.2
ALT (IU/L)	78.6 ± 60.8	78.1 ± 61.4	79.7 ± 59.6
GGT (IU/L)	59.3 ± 63.6	58.9 ± 62.0	60.2 ± 66.9
Platelets (10^9/L)	154 ± 53	153 ± 52	154 ± 56
Fibrosis: F3-4	121 (24%)	80 (24%)	41 (25%)
HCV-RNA: >600,000 IU/ml	409 (82%)	273 (82%)	136 (82%)
ISDR mutation: ≤1	220 (88%)	290 (88%)	145 (88%)
Core 70 (Arg/Gln or His)	293 (59%)/203 (41%)	197 (60%)/134 (40%)	96 (58%)/69 (42%)
Core 91 (Leu/Met)	299 (60%)/197 (40%)	200 (60%)/131 (40%)	99 (60%)/66 (40%)
IL28B: Minor allele	151 (30%)	101 (31%)	50 (30%)
SVR	194 (39%)	129 (39%)	65 (39%)
Relapse	152 (31%)	103 (31%)	49 (30%)
NVR	150 (30%)	99 (30%)	51 (31%)

ALT, alanine aminotransferase; GGT, gamma-glutamyltransferase; ISDR, interferon sensitivity determining region; Arg, arginine; Gln, glutamine; His, histidine; Leu, leucine; Met, methionine; Minor, heterozygote or homozygote of minor allele; SVR, sustained virological response; NVR, null virological response.

Japanese [6], European [7], and a multi-ethnic population [8,9]. The last three studies focused on the association of SNPs in the *IL28B* region with SVR [7–9] but we found a stronger association with NVR [6]. In addition to these host genetic factors, we have reported that mutations within a stretch of 40 amino acids in the NS5A region of HCV, designated as the IFN sensitivity determining region (ISDR), are closely associated with the virological response to IFN therapy: a lower number of mutations is associated with treatment failure [10–13]. Amino acid substitutions at positions 70 and 91 of the HCV core region (Core70, Core91) also have been reported to be associated with response to PEG-IFN/RBV therapy: glutamine (Gln) or histidine (His) at Core70 and methionine (Met) at Core91 are associated with treatment resistance [4,14]. The importance of substitutions in the HCV core and ISDR was confirmed recently by a Japanese multicenter study [15]. How these viral factors contribute to response to therapy is yet to be determined. For general application in clinical practice, host genetic factors and viral factors should be considered together.

Data mining analysis is a family of non-parametric regression methods for predictive modeling. Software is used to automatically explore the data to search for optimal split variables and to build a decision tree structure [16]. The major advantage of decision tree analysis over logistic regression analysis is that the results of the analysis are presented in the form of flow chart, which can be interpreted intuitively and readily made available for use in clinical practice [17]. The decision tree analysis has been utilized to define prognostic factors in various diseases [18–25]. We have reported recently its usefulness for the prediction of an early virological response (undetectable HCV-RNA within 12 weeks of therapy) to PEG-IFN/RBV therapy in chronic hepatitis C [26].

This study aimed to define the pre-treatment prediction of response to PEG-IFN/RBV therapy through the integrated analysis of host factors, such as the *IL28B* genetic polymorphism and various clinical covariates, as well as viral factors, such as mutations in the HCV core and ISDR and serum HCV-RNA load. In addition, for the general application of these results in clinical practice, decision models for the pre-treatment prediction of response were determined by data mining analysis.

Materials and methods

Patients

This was a multicentre retrospective study supported by the Japanese Ministry of Health, Labor and Welfare. Data were collected from a total of 496 chronic hepatitis C patients who were treated with PEG-IFN alpha and RBV at five hospitals and universities throughout Japan. Of these, 98 patients also were included in the original GWAS analysis [6]. The inclusion criteria in this study were as follows (1) infection by genotype 1b, (2) lack of co-infection with hepatitis B virus or human immunodeficiency virus, (3) lack of other causes of liver disease, such as autoimmune hepatitis, and primary biliary cirrhosis, (4) completion of at least 24 weeks of therapy, (5) adherence of more than 80% to the planned dose of PEG-IFN and RBV for the NVR patients, (6) availability of DNA for the analysis of the genetic polymorphism of *IL28B*, and (7) availability of serum for the determination of mutations in the ISDR and substitutions of Core70 and Core91 of HCV. Patients received PEG-IFN alpha-2a (180 μg) or 2b (1.5 μg/kg) subcutaneously every week and were administered a weight adjusted dose of RBV (600 mg for <60 kg, 800 mg for 60–80 kg, and 1000 mg for >80 kg daily) which is the recommended dosage in Japan. Written informed consent was obtained from each patient and the study protocol conformed to the ethical guidelines of the Declaration of Helsinki and was approved by the institutional ethics review committee. The baseline characteristics are listed in Table 1. For the data mining analysis, 67% of the patients (331 patients) were assigned randomly to the model building group and 33% (165 patients) to the validation group. There were no significant differences in the clinical backgrounds between these two groups.

Laboratory and histological tests

Blood samples were obtained before therapy and were analyzed for hematologic tests and for blood chemistry and HCV-RNA. Sequences of ISDR and the core region of HCV were determined by direct sequencing after amplification by reverse-transcription and polymerase chain reaction as reported previously [4,11]. Genetic polymorphism in one tagging SNP located near the *IL28B* gene (rs8099917) was determined by the GWAS or DigiTag2 assay [27]. Homozygosity (GG) or heterozygosity (TG) of the minor sequence was defined as having the *IL28B* minor allele, whereas homozygosity for the major sequence (TT) was

JOURNAL OF **HEPATOLOGY**

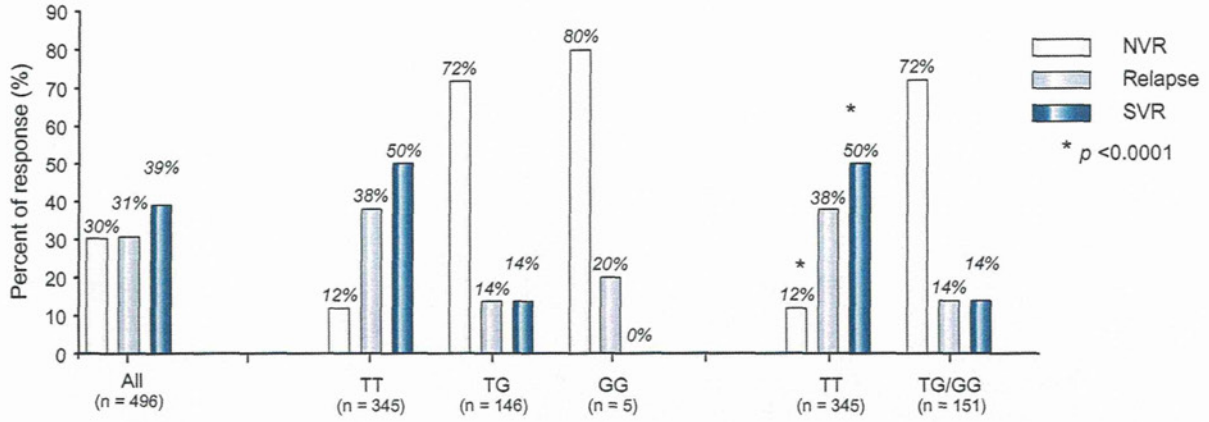

Fig. 1. Association between the IL28B genotype (rs8099917) and treatment response. The rates of response to treatment are shown for each rs8099917 genotype. The rate of null virological response (NVR), relapse, and sustained virological response (SVR) is shown. The *p* values are from Fisher's exact test. The rate of NVR was significantly higher ($p < 0.0001$) and the rate of SVR was significantly lower ($p < 0.0001$) in patients with the *IL28B* minor allele compared to those with the major allele.

defined as having the *IL28B* major allele. In this study, NVR was defined as a less than 2 log reduction of HCV-RNA at week 12 and detectable HCV-RNA by qualitative PCR with a lower detection limit of 50 IU/ml (Amplicor, Roche Diagnostic systems, CA) at week 24 during therapy. RVR (rapid virological response) and complete early virological response (cEVR) were defined as undetectable HCV-RNA at 4 weeks and 12 weeks during therapy and SVR was defined as undetectable HCV-RNA 24 weeks after the completion of therapy. Relapse was defined as reappearance of HCV-RNA after the completion of therapy. The stage of liver fibrosis was scored according to the METAVIR scoring system: F0 (no fibrosis), F1 (mild fibrosis: portal fibrosis without septa), F2 (moderate fibrosis: few septa), F3 (severe fibrosis: numerous septa without cirrhosis) and F4 (cirrhosis). Percentage of steatosis was quantified in 111 patients by determining the average proportion of hepatocytes affected by steatosis.

Statistical analysis

Associations between pre-treatment variables and treatment response were analyzed by univariate and multivariate logistic regression analysis. Associations between the *IL28B* polymorphism and sequences of HCV were analyzed by Fisher's exact test. SPSS software v.15.0 (SPSS Inc., Chicago, IL) was used for these analyses. For the data mining analysis, IBM-SPSS Modeler version 13.0 (IBM-SPSS Inc., Chicago, IL) software was utilized as reported previously [26]. The patients used for model building were divided into two groups at each step of the analysis based on split variables. Each value of each variable was considered as a potential split. The optimum variables and cut-off values were determined by a statistical search algorithm to generate the most significant division into two prognostic subgroups that were as homogeneous as possible for the probability of SVR. Thereafter, each subgroup was evaluated again and divided further into subgroups. This procedure was repeated until no additional significant variable was detected or the sample size was below 15. To avoid over-fitting, 10-fold cross validation was used in the tree building process. The reproducibility of the resulting model was tested with the data from the validation patients.

Results

Association between the IL28B (rs8099917) genotype and the PEG-IFN/RBV response

The rs8099917 allele frequency was 70% for TT ($n = 345$), 29% for TG ($n = 146$), and 1% for GG ($n = 5$). We defined the *IL28B* major allele as homozygous for the major sequence (TT) and the *IL28B* minor allele as homozygous (GG) or heterozygous (TG) for the minor sequence. The rate of NVR was significantly higher (72% vs. 12%, $p < 0.0001$) and the rate of SVR was significantly lower (14% vs. 50%, $p < 0.0001$) in patients with the *IL28B* minor allele compared to those with the major allele (Fig. 1).

Effect of the IL28B polymorphism, substitutions in the ISDR, Core70, and Core91 of HCV on time-dependent clearance of HCV

Patients were stratified according to their *IL28B* allele type, the number of mutations in the ISDR, the amino acid substitutions in Core70 and Core91, and the rate of undetectable HCV-RNA at 4, 8, 12, 24, and 48 weeks after the start of therapy were analyzed (Fig. 2A–D). The rate of undetectable HCV-RNA was significantly higher in patients with the *IL28B* major allele than the minor allele, in patients with two or more mutations in the ISDR compared to none or only one mutation, in patients with arginine (Arg) at Core70 rather than Gln/His, and in patients with leucine (Leu) at Core91 rather than Met. The difference was most significant when stratified by the *IL28B* allele type. The rate of RVR and cEVR was significantly more frequent in patients with the *IL28B* major allele compared with those with the *IL28B* minor allele: 9% vs. 3% for RVR ($p < 0.005$) and 57% vs. 11% for cEVR ($p < 0.0001$). These findings suggest that *IL28B* has the greatest impact on early virological response to therapy.

Association between substitutions in the ISDR and relapse after the completion of therapy

Patients were stratified according to the *IL28B* allele, number of mutations in the ISDR, and amino acid substitutions of Core70 and Core91, and the rate of relapse was analyzed (Fig. 3A and B). Among patients who achieved cEVR, the rate of relapse was significantly lower in patients with two or more mutations in the ISDR compared to those with only one or no mutations (15% vs. 31%, $p < 0.005$) (Fig. 3 B). On the other hand, the relapse rate was not different between the *IL28B* major and minor alleles within patients who achieved RVR (3% vs. 0%) or cEVR (28% vs. 29%) (Fig. 3A). Amino acid substitutions of Core70 and Core91 were not associated with the rate of relapse (data not shown).

Factors associated with response by multivariate logistic regression analysis

By univariate analysis, the minor allele of *IL28B* ($p < 0.0001$), one or no mutations in the ISDR ($p = 0.03$), high serum level of

Research Article

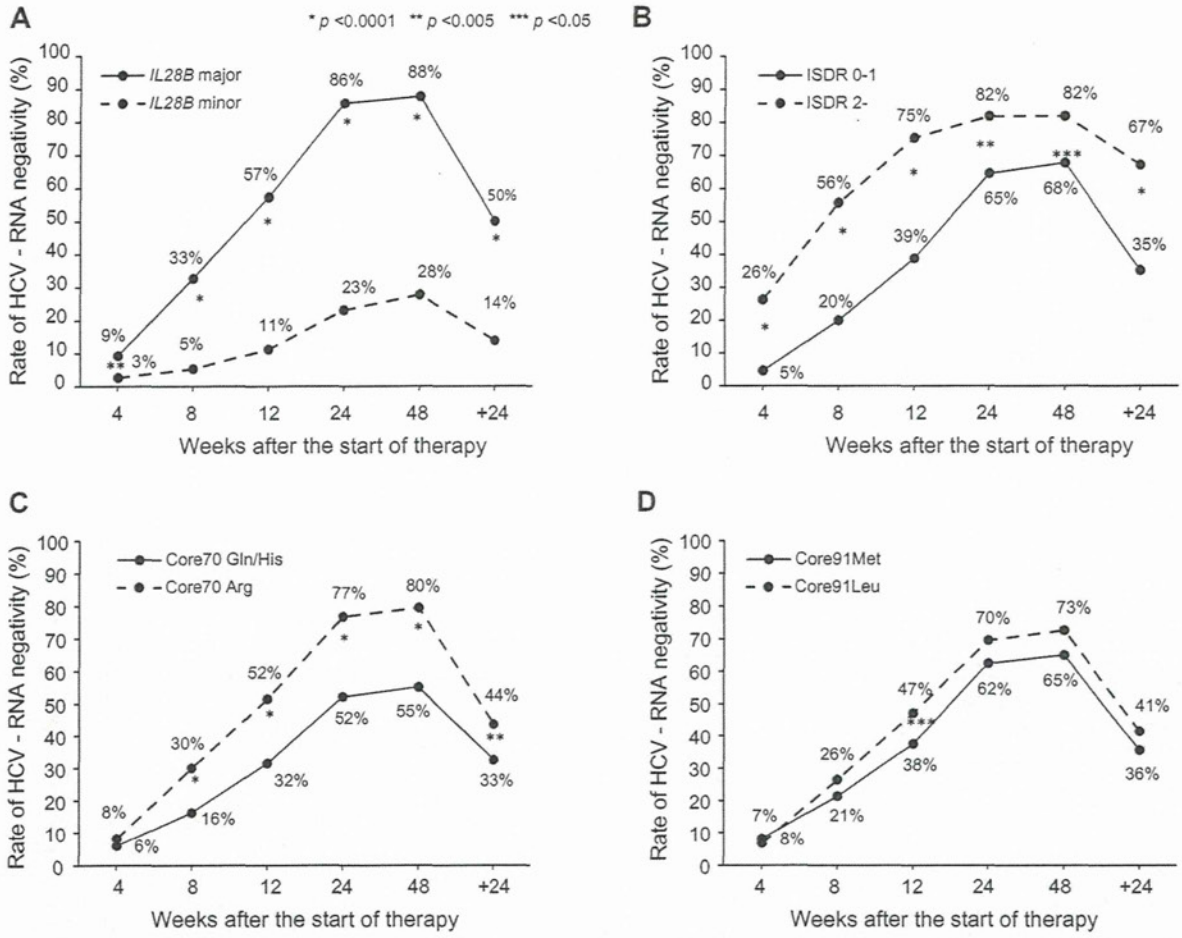

Fig. 2. Effect of *IL28B* mutations in the ISDR, Core70, and Core91 of HCV on time-dependent clearance of HCV. The rate of undetectable HCV-RNA was plotted for serial time points after the start of therapy (4, 8, 12, 24, and 48 weeks) and for 24 weeks after the completion of therapy. Patients were stratified according to (A) the *IL28B* allele (minor allele vs. major allele), (B) the number of mutations in the ISDR (0–1 mutation vs. 2 or more mutations), amino acid substitutions of (C) Core70 (Gln/His vs. Arg), and (D) Core91 (Met vs. Leu). The *p* values are from Fisher's exact test.

HCV-RNA ($p = 0.035$), Gln or His at Core70 ($p < 0.0001$), low platelet counts ($p = 0.009$), and advanced fibrosis ($p = 0.0002$) were associated with NVR. By multivariate analysis, the minor allele of *IL28B* (OR = 20.83, 95%CI = 11.63–37.04, $p < 0.0001$) was associated with NVR independent of other covariates (Table 2). Notably, mutations in the ISDR ($p = 0.707$) and at amino acid Core70 ($p = 0.207$) were not significant in multivariate analysis due to the positive correlation with the *IL28B* polymorphism ($p = 0.004$ for ISDR and $p < 0.0001$ for Core70, Fig. 4).

Genetic polymorphism of *IL28B* also was associated with SVR (OR = 7.41, 95% CI = 4.05–13.57, $p < 0.0001$) independent of other covariates, such as platelet counts, fibrosis, and serum levels of HCV-RNA. Mutation in the ISDR was an independent predictor of SVR (OR = 2.11, 95% CI = 1.06–4.18, $p = 0.033$) but the amino acid at Core70 was not (Table 3).

Factors associated with the IL28B polymorphism

Patients with the *IL28B* minor allele had significantly higher serum level of gamma-glutamyltransferase (GGT) and a higher frequency of hepatic steatosis (Table 4). When the association between the *IL28B* polymorphism and HCV sequences was analyzed, Gln or His at Core70, that is linked to resistance to PEG-IFN and RBV therapy [4,14,15], was significantly more frequent in patients with the minor *IL28B* allele than in those with the major allele (67% vs. 30%, $p < 0.0001$) (Fig. 4). Other HCV sequences with an IFN resistant phenotype also were more prevalent in patients with the minor *IL28B* allele than those with the major allele: Met at Core91 (46% vs. 37%, $p = 0.047$) and one or no mutations in the ISDR (94% vs. 85%, $p = 0.004$) (Fig. 4).

Data mining analysis

Data mining analysis was performed to build a model for the prediction of SVR and the result is shown in Fig. 5. The analysis selected four predictive variables, resulting in six subgroups of patients. Genetic polymorphism of *IL28B* was selected as the best predictor of SVR. Patients with the minor *IL28B* allele had a lower probability of SVR and a higher probability of NVR than those with the major *IL28B* allele (SVR: 14% vs. 50%, NVR: 72% vs.

JOURNAL OF **HEPATOLOGY**

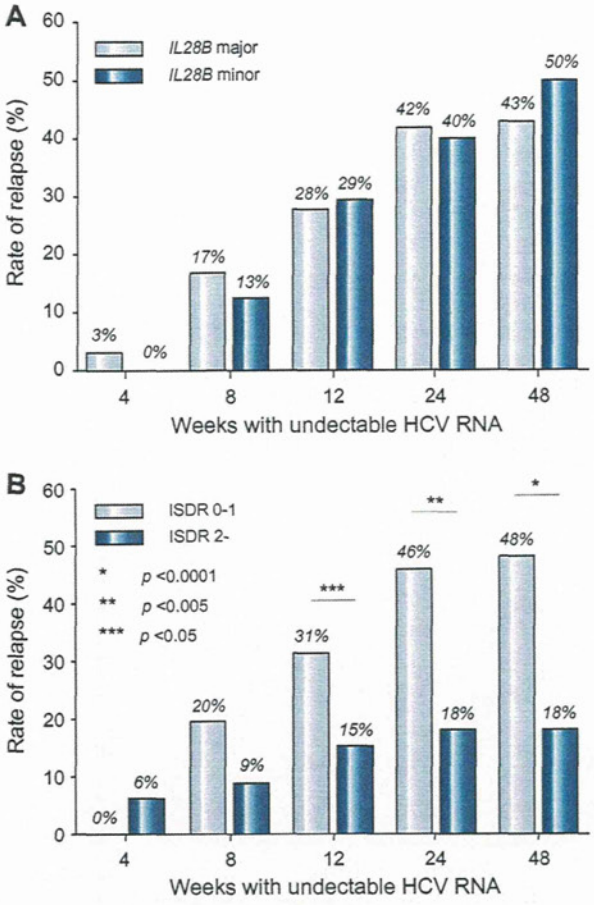

Fig. 3. Association between relapse and the *IL28B* allele or mutations in the ISDR. The rate of relapse was calculated for patients who had undetectable HCV-RNA at serial time points after the start of therapy (4, 8, 12, 24, and 48 weeks). Patients were stratified according to (A) the *IL28B* allele (minor allele vs. major allele) and (B) the number of mutations in the ISDR (0–1 mutation vs. 2 or more mutations). The *p* values are from Fisher's exact test.

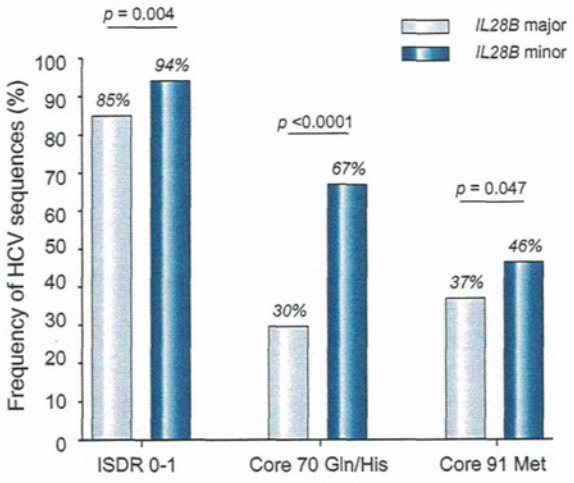

Fig. 4. Associations between the *IL28B* allele and HCV sequences. The prevalence of HCV sequences predicting a resistant phenotype to IFN was higher in patients with the minor *IL28B* allele than those with major allele. (A) 0 or 1 mutation in the ISDR of NS5A, (B) Gln or His at Core70, and (C) Met at Core91. *p* values are from Fisher's exact test.

12%). After stratification by the *IL28B* allele, patients with low platelet counts (<140 × 10^9/L) had a lower probability of SVR and higher probability of NVR than those with high platelet counts (⩾140 × 10^9/L): for the minor *IL28B* allele, SVR was 7% vs. 19%, and NVR was 84% vs. 62%, and for the major *IL28B* allele, SVR was 32% vs. 66% and NVR was 16% vs. 8%. Among patients with the major *IL28B* allele and low platelet counts, those with two or more mutations in the ISDR had a higher probability of SVR and lower probability of relapse than those with one or no mutations in the ISDR (SVR: 75% vs. 27%, and relapse: 8% vs. 57%). Among patients with the major *IL28B* allele and high platelet counts, those with a low HCV-RNA titer (<600,000 IU/ml) had a higher probability of SVR and lower probability of NVR and relapse than those with a high HCV-RNA titer (SVR: 90% vs. 61%, NVR: 0% vs. 10%, and relapse: 10% vs. 29%). The sensitivity and specificity of the decision tree were 78% and 70%, respectively. The area under the receiver operating characteristic (ROC) curve of the model was 0.782 (data not shown). The proportion of patients with advanced fibrosis (F3-4) was 39% (84/217) in patients with low platelet counts (<140 × 10^9/L) compared to 13% (37/279) in those with high platelet counts (⩾140 × 10^9/L).

Validation of the data mining analysis

The results of the data mining analysis were validated with 165 patients who differed from those used for model building. Each patient was allocated to one of the six subgroups for the validation using the flow-chart form of the decision tree. The rate of SVR and NVR in each subgroup was calculated. The rates of SVR and NVR for each subgroup of patients were closely correlated between the model building and the validation patients (r^2 = 0.99 and 0.98) (Fig. 6).

Discussion

The rate of NVR after 48 weeks of PEG-IFN/RBV therapy among patients infected with HCV of genotype 1 is around 20–30%. Previously, there have been no reliable baseline predictors of NVR or SVR. Because more potent therapies, such as protease and polymerase inhibitor of HCV [28,29] and nitazoxianide [30], are in clinical trials and may become available in the near future, a pre-treatment prediction of the likelihood of response may be helpful for patients and physicians, to support clinical decisions about whether to begin the current standard of care or whether to wait for emerging therapies. This study revealed that the *IL28B* polymorphism was the overwhelming predictor of NVR and is independent of host factors and viral sequences reported previously. The *IL28B* encodes a protein also known as IFN-lambda 3, which is thought to suppress the replication of various viruses including HCV [31,32]. The results of the current study and the findings of the GWAS studies [6–9] may provide the rationale for developing diagnostic testing or an IFN-lambda based therapy for chronic hepatitis C in the future.

Research Article

Table 2. Factors associated with NVR analyzed by univariate and multivariate logistic regression analysis.

	Univariate			Multivariate		
	Odds ratio	95%CI	*p* value	Odds ratio	95%CI	*p* value
Gender: female	0.98	0.67-1.45	0.938	1.29	0.75-2.23	0.363
Age	1.01	0.97-1.01	0.223	0.99	0.97-1.02	0.679
ALT	1.00	1.00-1.00	0.867	1.00	0.99-1.00	0.580
GGT	1.004	1.00-1.01	0.029	1.00	1.00-1.00	0.715
Platelets	0.95	0.91-0.99	0.009	0.92	0.87-0.98	0.006
Fibrosis: F3-4	2.23	1.46-3.42	0.0002	1.97	1.09-3.57	0.025
HCV-RNA: ≥600,000 IU/ml	1.83	1.05-3.19	0.035	2.49	1.17-5.29	0.018
ISDR mutation: ≤1	2.14	1.08-4.22	0.030	0.96	0.78-1.18	0.707
Core 70 (Gln/His)	3.23	2.16-4.78	<0.0001	1.41	0.83-2.42	0.207
Core 91 (Met)	1.39	0.95-2.06	0.093	1.21	0.72-2.04	0.462
IL28B: Minor allele	19.24	11.87-31.18	<0.0001	20.83	11.63-37.04	<0.0001

ALT, alanine aminotransferase; GGT, gamma-glutamyltransferase; ISDR, interferon sensitivity determining region; Gln, glutamine; His, histidine; Met, methionine; Minor allele, heterozygote or homozygote of minor allele.

Table 3. Factors associated with SVR analyzed by univariate and multivariate logistic regression analysis.

	Univariate			Multivariate		
	Odds ratio	95%CI	*p* value	Odds ratio	95%CI	*p* value
Gender: female	0.81	0.56-1.16	0.253	0.86	0.55-1.35	0.508
Age	0.97	0.95-0.99	0.0003	0.99	0.96-1.01	0.199
ALT	1.00	1.00-1.00	0.337	1.00	1.00-1.01	0.108
GGT	1.00	1.00-1.00	0.273	1.00	1.00-1.00	0.797
Platelets	1.12	1.01-116	<0.0001	1.13	1.08-1.19	<0.0001
Fibrosis: F0-2	2.64	1.65-4.22	<0.0001	1.87	1.07-3.28	0.029
HCV-RNA: <600,000 IU/ml	2.49	1.55-3.98	0.0001	2.75	1.55-4.90	0.001
ISDR mutation: 2≤	3.78	2.14-6.68	<0.0001	2.11	1.06-4.18	0.033
Core 70 (Arg)	1.61	1.11-2.28	0.012	0.84	0.52-1.35	0.470
Core 91 (Leu)	1.28	0.88-1.85	0.185	1.26	0.81-1.96	0.300
IL28B: Major allele	6.21	3.75-10.31	<0.0001	7.41	4.05-13.57	<0.0001

ALT, alanine aminotransferase; GGT, Gamma-glutamyltransferase; ISDR, interferon sensitivity determining region; Arg, arginine; Leu, leucine; Major allele, homozygote of major allele.

Among baseline factors, *IL28B* was the most significant predictor of NVR and SVR. Moreover, the *IL28B* allele type was also correlated with early virological response: the rate of RVR and cEVR was significantly high for the *IL28B* major allele compared to the *IL28B* minor allele: 9% vs. 3% for RVR and 57% vs. 11% for cEVR (Fig. 2). On the other hand, the relapse rate was not different between the *IL28B* genotypes within patients who achieved RVR or cEVR (Fig. 3). We believe that optimal therapy should be based on baseline features and a response-guided approach. Our findings suggest that the *IL28B* genotype is a useful baseline predictor of virological response which should be used for selecting the treatment regimen: whether to treat patients with PEG-IFN and RBV or to wait for more effective future therapy including direct acting antiviral drugs. On the other hand, baseline *IL28B* genotype might not be suitable for determining the treatment duration in patients who started PEG-IFN/RBV therapy and whose virological response is determined because the *IL28B* genotype is not useful for the prediction of relapse. The duration of therapy should be personalized based on the virological response. Future studies need to explore whether the combination of baseline *IL28B* genotype and response-guided approach further improves the optimization of treatment duration.

The SVR rate in patients having the *IL28B* minor allele was 14% in the present study while it was 23% in Caucasians and 9% in African Americans in a study by McCarthy et al. [33]. On the other hand, the SVR rate in patients having the *IL28B* minor allele was 28% in genotypes 1/4 compared to 80% in genotypes 2/3 in a study by Rauch et al. [9]. These data imply that the impact of the *IL28B* polymorphism on response to therapy may be different in terms of race, geographical areas, or HCV genotypes, and that our data need to be validated in future studies including different populations and geographical areas before generalization.

Table 4. Factors associated with IL28B genotype.

	IL28B major allele n = 345	*IL28B* minor allele n = 151	*p* value
Gender: male	166 (48%)	84 (56%)	0.143
Age (years)	57 ± 10	57 ± 10	0.585
ALT (IU/L)	79 ± 60	78 ± 62	0.842
Platelets (10^9/L)	153 ± 54	155 ± 52	0.761
GGT (IU/L)	51 ± 45	78 ± 91	0.001
Fibrosis: F3-4	76 (22%)	45 (30%)	0.063
Steatosis:			
>10%	16/88 (18%)	13/23 (57%)	0.024
>30%	6/88 (7%)	6/23 (26%)	0.017
HCV-RNA: >600,000 IU/ml	284 (82%)	125 (83%)	1.000

ALT, alanine aminotransferase; GGT, gamma-glutamyltransferase.

Four GWAS studies have shown the association between a genetic polymorphism near the *IL28B* gene and response to PEG-IFN plus RBV therapy. The SNPs that showed significant association with response were rs12979860 [8] and rs8099917 [6,7,9]. There is a strong linkage-disequilibrium (LD) between these two SNPs as well as several other SNPs near the *IL28B* gene in Japanese patients [34] but the degree of LD was weaker in Caucasians and Hispanics [8]. Thus, the combination of SNPs is not useful for predicting response in Japanese patients but may improve the predictive value in patients other than Japanese who have weaker LD between SNPs.

Other significant predictors of response independent of *IL28B* genotype were platelet counts, stage of fibrosis, and HCV RVA load. A previous study reported that platelet count is a predictor of response to therapy [35], and the lower platelet count was related with advanced liver fibrosis in the present study. The association between response to therapy and advanced fibrosis independent of the *IL28B* polymorphism is consistent with a recent study by Rauch et al. [9].

There is agreement that the viral genotype is significantly associated with the treatment outcome. Moreover, viral factors such as substitutions in the ISDR of the NS5A region [10] or in the amino acid sequence of the HCV core [4] have been studied in relation to the response to IFN treatment. The amino acid Gln or His at Core70 and Met at Core91 are repeatedly reported to be associated with resistance to therapy [4,14,15] in Japanese patients but these data wait to be validated in different populations or other geographical areas. In this study, we confirmed that patients with two or more mutations in the ISDR had a higher rate of undetectable HCV-RNA at each time point during therapy. In addition, the rate of relapse among patients who achieved cEVR was significantly lower in patients with two or more mutations in ISDR compared to those with only one or no mutations (15% vs. 31%, $p < 0.05$). Thus, the ISDR sequence may be used to predict a relapse among patients who achieved virological response during therapy, while the *IL28B* polymorphism may be used to predict the virological response before therapy. A higher number of mutations in the ISDR are reported to have close association with SVR in Japanese [11–13,15,36] or Asian [37,38] populations but data from Western countries have been controversial [39–42]. A meta-analysis of 1230 patients including 525 patients from Europe has shown that there was a positive correlation between the SVR and the number of mutations in the ISDR in Japanese as well as in European patients [43] but this correlation was more pronounced in Japanese patients. Thus, geographical factors may account for the different impact of ISDR on treatment response, which may be a potential limitation of our study.

To our surprise, these HCV sequences were associated with the *IL28B* genotype: HCV sequences with an IFN resistant phenotype were more prevalent in patients with the minor IL28B allele than those with the major allele. This was an unexpected finding, as we initially thought that host genetics and viral sequences were completely independent. A recent study reported that the *IL28B* polymorphism (rs12979860) was significantly associated with HCV genotype: the *IL28B* minor allele was more frequent in HCV genotype 1-infected patients compared to patients infected with HCV genotype 2 or 3 [33]. Again, patients with the *IL28B* minor allele (IFN resistant genotype) were infected with HCV sequences that are linked to an IFN resistant phenotype. The mechanism for this association is unclear, but may be related to an interaction between the *IL28B* genotype and HCV sequences in the development of chronic HCV infection as discussed by McCarthy et al., since the *IL28B* polymorphism was associated with the natural clearance of HCV [44]. Alternatively, the HCV sequence within the patient may be selected during the course of chronic infection [45,46]. These hypotheses should be explored through prospective studies of spontaneous HCV clearance or by testing the time-dependent changes in the HCV sequence during the course of chronic infection.

How these host and viral factors can be integrated to predict the response to therapy in future clinical practice is an important question. Because various host and viral factors interact in the same patient, predictive analysis should consider these factors in combination. Using the data mining analysis, we constructed a simple decision tree model for the pre-treatment prediction of SVR and NVR to PEG-IFN/RBV therapy. The classification of patients based on the genetic polymorphism of *IL28B*, mutation in the ISDR, serum levels of HCV-RNA, and platelet counts, identified subgroups of patients who have the lowest probabilities of NVR (0%) with the highest probabilities of SVR (90%) as well as those who have the highest probabilities of NVR (84%) with the lowest probability of SVR (7%). The reproducibility of the model was confirmed by the independent validation based on a second group of patients. Using this model, we can rapidly develop an

Research Article

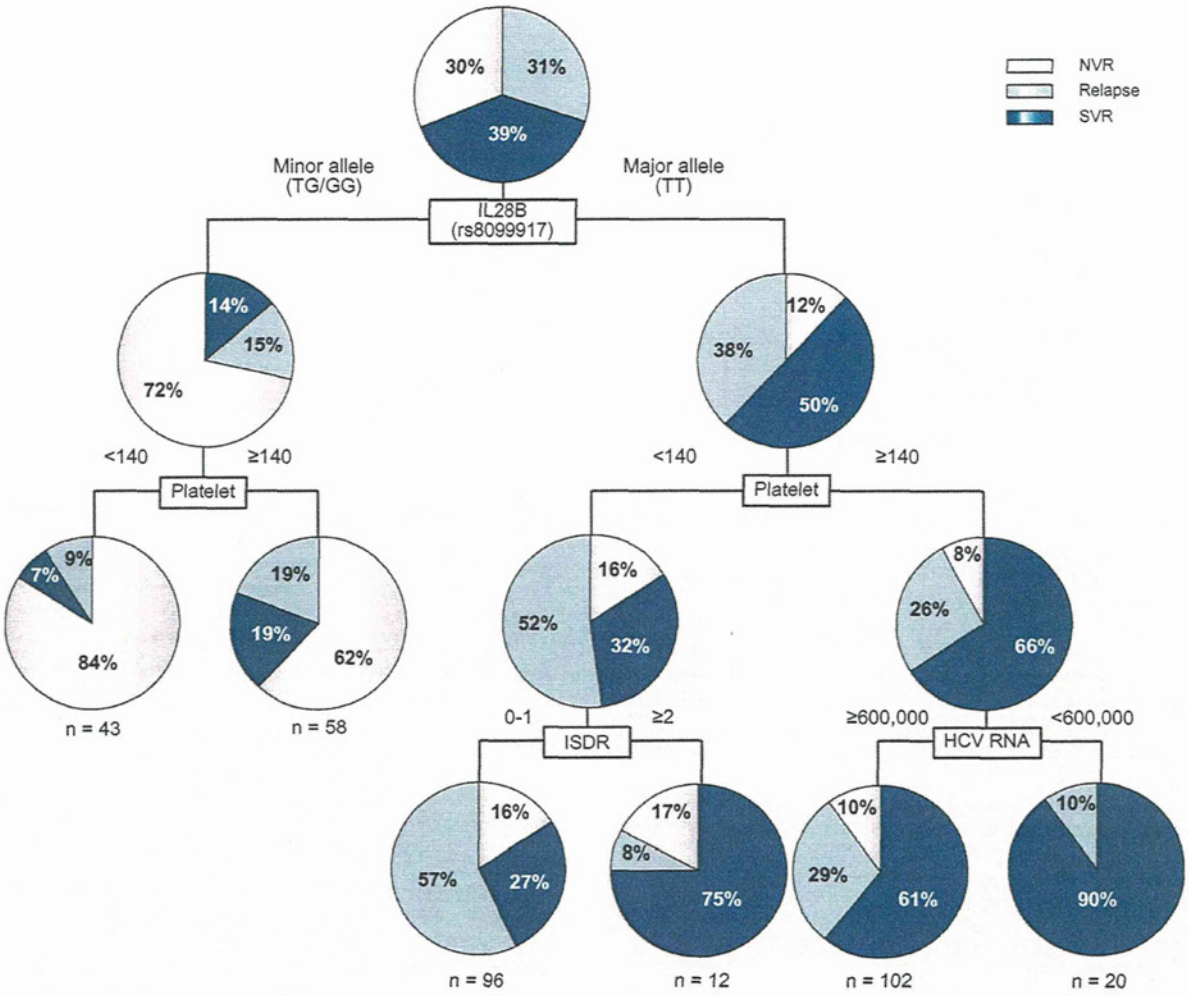

Fig. 5. Decision tree for the prediction of response to therapy. The boxes indicate the factors used for splitting. Pie charts indicate the rate of response for each group of patients after splitting. The rate of null virological response, relapse, and sustained virological response is shown.

estimate of the response before treatment, by simply allocating patients to subgroups by following the flow-chart form, which may facilitate clinical decision making. This is in contrast to the calculating formula, which was constructed by the traditional logistic regression model. This was not widely used in clinical practice as it is abstruse and inconvenient. These results support the evidence based approach of selecting the optimum treatment strategy for individual patients, such as treating patients with a low probability of NVR with current PEG-IFN/RBV combination therapy or advising those with a high probability of NVR to wait for more effective future therapies. Patients with a high probability of relapse may be treated for a longer duration to avoid a relapse. Decisions may be based on the possibility of a response against a potential risk of adverse events and the cost of the therapy, or disease progression while waiting for future therapy.

We have previously reported the predictive model of early virological response to PEG-IFN and RBV in chronic hepatitis C [26]. The top factor selected as significant was the grade of steatosis, followed by serum level of LDL cholesterol, age, GGT, and blood sugar. The mechanism of association between these factors and treatment response was not clear at that time. To our interest, a recent study by Li et al. [47] has shown that high serum level of LDL cholesterol was linked to the *IL28B* major allele (CC in rs12979860). High serum level of LDL cholesterol was associated with SVR but it was no longer significant when analyzed together with the *IL28B* genotype in multivariate analysis. Thus, the association between treatment response and LDL cholesterol levels may reflect the underlining link of LDL cholesterol levels to *IL28B* genotype. Steatosis is reported to be correlated with low lipid levels [48] which suggest that *IL28B* genotypes may be also associated with steatosis. In fact, there were significant correlations between the *IL28B* genotype and the presence of steatosis in the present study (Table 4). In addition, the serum level of GGT, another predictive factor in our previous study, was signif-

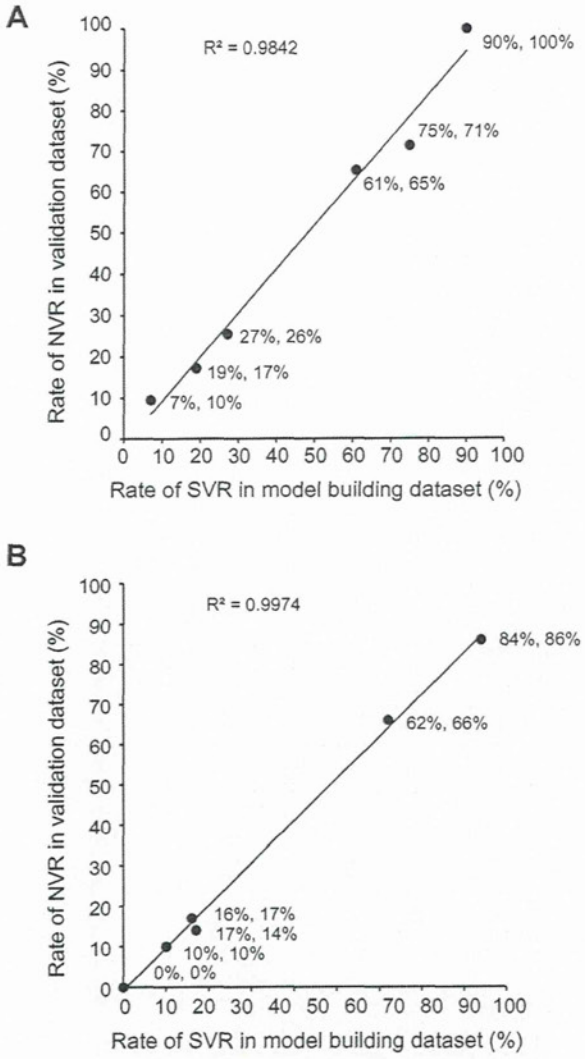

Fig. 6. Validation of the CART analysis. Each patient in the validation group was allocated to one of the six subgroups by following the flow-chart form of the decision tree. The rate of (A) sustained virological response (SVR) and (B) null virological response (NVR) in each subgroup was calculated and plotted. The *X*-axis represents the rate of SVR or NVR in the model building patients and the *Y*-axis represents those in the validation patients. The rate of SVR and NVR in each subgroup of patients is closely correlated between the model building and the validation patients (correlation coefficient: $r^2 = 0.98–0.99$).

icantly associated with *IL28B* genotype in the present study (Table 4). The serum level of GGT was significantly associated with NVR when examined independently but was no longer significant when analyzed together with the *IL28B* genotype. These observations indicate that some of the factors that we have previously identified may be associated with virological response to therapy through the underlining link to the *IL28B* genotype.

In conclusion, the present study highlighted the impact of the *IL28B* polymorphism and mutation in the ISDR on the pre-treatment prediction of response to PEG-IFN/RBV therapy. A decision model including these host and viral factors has the potential to support selection of the optimum treatment strategy for individual patients, which may enable personalized treatment.

Conflict of interest

The authors who have taken part in this study declare that they do not have anything to disclose regarding funding or conflict of interest with respect to this manuscript.

Financial support

This study was supported by a grant-in-aid from the Ministry of Health, Labor and Welfare, Japan, (H19-kannen-013), (H20-kannen-006).

References

[1] Ray Kim W. Global epidemiology and burden of hepatitis C. Microbes Infect 2002;4 (12):1219–1225.
[2] Fried MW, Shiffman ML, Reddy KR, Smith C, Marinos G, Goncales Jr FL, et al. Peginterferon alfa-2a plus ribavirin for chronic hepatitis C virus infection. N Engl J Med 2002;347 (13):975–982.
[3] Manns MP, McHutchison JG, Gordon SC, Rustgi VK, Shiffman M, Reindollar R, et al. Peginterferon alfa-2b plus ribavirin compared with interferon alfa-2b plus ribavirin for initial treatment of chronic hepatitis C: a randomised trial. Lancet 2001;358 (9286):958–965.
[4] Akuta N, Suzuki F, Sezaki H, Suzuki Y, Hosaka T, Someya T, et al. Association of amino acid substitution pattern in core protein of hepatitis C virus genotype 1b high viral load and non-virological response to interferon-ribavirin combination therapy. Intervirology 2005;48 (6):372–380.
[5] Davis GL, Wong JB, McHutchison JG, Manns MP, Harvey J, Albrecht J. Early virologic response to treatment with peginterferon alfa-2b plus ribavirin in patients with chronic hepatitis C. Hepatology 2003;38 (3):645–652.
[6] Tanaka Y, Nishida N, Sugiyama M, Kurosaki M, Matsuura K, Sakamoto N, et al. Genome-wide association of IL28B with response to pegylated interferon-alpha and ribavirin therapy for chronic hepatitis C. Nat Genet 2009;10:1105–1109.
[7] Suppiah V, Moldovan M, Ahlenstiel G, Berg T, Weltman M, Abate ML, et al. IL28B is associated with response to chronic hepatitis C interferon-alpha and ribavirin therapy. Nat Genet 2009;10:1100–1104.
[8] Ge D, Fellay J, Thompson AJ, Simon JS, Shianna KV, Urban TJ, et al. Genetic variation in IL28B predicts hepatitis C treatment-induced viral clearance. Nature 2009;461 (7262):399–401.
[9] Rauch A, Kutalik Z, Descombes P, Cai T, Di Iulio J, Mueller T, et al. Genetic variation in IL28B is associated with chronic hepatitis C and treatment failure: a genome-wide association study. Gastroenterology 2010;138 (4):1338–1345.
[10] Enomoto N, Sakuma I, Asahina Y, Kurosaki M, Murakami T, Yamamoto C, et al. Comparison of full-length sequences of interferon-sensitive and resistant hepatitis C virus 1b. Sensitivity to interferon is conferred by amino acid substitutions in the NS5A region. J Clin Invest 1995;96 (1):224–230.
[11] Enomoto N, Sakuma I, Asahina Y, Kurosaki M, Murakami T, Yamamoto C, et al. Mutations in the nonstructural protein 5A gene and response to interferon in patients with chronic hepatitis C virus 1b infection. N Engl J Med 1996;334 (2):77–81.
[12] Kurosaki M, Enomoto N, Murakami T, Sakuma I, Asahina Y, Yamamoto C, et al. Analysis of genotypes and amino acid residues 2209 to 2248 of the NS5A region of hepatitis C virus in relation to the response to interferon-beta therapy. Hepatology 1997;25 (3):750–753.
[13] Shirakawa H, Matsumoto A, Joshita S, Komatsu M, Tanaka N, Umemura T, et al. Pretreatment prediction of virological response to peginterferon plus ribavirin therapy in chronic hepatitis C patients using viral and host factors. Hepatology 2008;48 (6):1753–1760.
[14] Akuta N, Suzuki F, Kawamura Y, Yatsuji H, Sezaki H, Suzuki Y, et al. Predictive factors of early and sustained responses to peginterferon plus ribavirin combination therapy in Japanese patients infected with hepatitis C virus genotype 1b: amino acid substitutions in the core region and low-density lipoprotein cholesterol levels. J Hepatol 2007;46 (3):403–410.

Research Article

[15] Okanoue T, Itoh Y, Hashimoto H, Yasui K, Minami M, Takehara T, et al. Predictive values of amino acid sequences of the core and NS5A regions in antiviral therapy for hepatitis C: a Japanese multi-center study. J Gastroenterol 2009;44 (9):952–963.

[16] Segal MR, Bloch DA. A comparison of estimated proportional hazards models and regression trees. Stat Med 1989;8 (5):539–550.

[17] LeBlanc M, Crowley J. A review of tree-based prognostic models. Cancer Treat Res 1995;75:113–124.

[18] Garzotto M, Beer TM, Hudson RG, Peters L, Hsieh YC, Barrera E, et al. Improved detection of prostate cancer using classification and regression tree analysis. J Clin Oncol 2005;23 (19):4322–4329.

[19] Averbook BJ, Fu P, Rao JS, Mansour EG. A long-term analysis of 1018 patients with melanoma by classic Cox regression and tree-structured survival analysis at a major referral center: implications on the future of cancer staging. Surgery 2002;132 (4):589–602.

[20] Leiter U, Buettner PG, Eigentler TK, Garbe C. Prognostic factors of thin cutaneous melanoma: an analysis of the central malignant melanoma registry of the german dermatological society. J Clin Oncol 2004;22 (18):3660–3667.

[21] Valera VA, Walter BA, Yokoyama N, Koyama Y, Iiai T, Okamoto H, et al. Prognostic groups in colorectal carcinoma patients based on tumor cell proliferation and classification and regression tree (CART) survival analysis. Ann Surg Oncol 2007;14 (1):34–40.

[22] Zlobec I, Steele R, Nigam N, Compton CC. A predictive model of rectal tumor response to preoperative radiotherapy using classification and regression tree methods. Clin Cancer Res 2005;11 (15):5440–5443.

[23] Thabane M, Simunovic M, Akhtar-Danesh N, Marshall JK. Development and validation of a risk score for post-infectious irritable bowel syndrome. Am J Gastroenterol 2009;104 (9):2267–2274.

[24] Wu BU, Johannes RS, Sun X, Tabak Y, Conwell DL, Banks PA. The early prediction of mortality in acute pancreatitis: a large population-based study. Gut 2008;57 (12):1698–1703.

[25] Fonarow GC, Adams Jr KF, Abraham WT, Yancy CW, Boscardin WJ. Risk stratification for in-hospital mortality in acutely decompensated heart failure: classification and regression tree analysis. Jama 2005;293 (5):572–580.

[26] Kurosaki M, Matsunaga K, Hirayama I, Tanaka T, Sato M, Yasui Y, et al. A predictive model of response to peginterferon ribavirin in chronic hepatitis C using classification and regression tree analysis. Hepatol Res 2010;40 (3):251–260.

[27] Nishida N, Tanabe T, Takasu M, Suyama A, Tokunaga K. Further development of multiplex single nucleotide polymorphism typing method, the DigiTag2 assay. Anal Biochem 2007;364 (1):78–85.

[28] Hezode C, Forestier N, Dusheiko G, Ferenci P, Pol S, Goeser T, et al. Telaprevir and peginterferon with or without ribavirin for chronic HCV infection. N Engl J Med 2009;360 (18):1839–1850.

[29] McHutchison JG, Everson GT, Gordon SC, Jacobson IM, Sulkowski M, Kauffman R, et al. Telaprevir with peginterferon and ribavirin for chronic HCV genotype 1 infection. N Engl J Med 2009;360 (18):1827–1838.

[30] Rossignol JF, Elfert A, El-Gohary Y, Keeffe EB. Improved virologic response in chronic hepatitis C genotype 4 treated with nitazoxanide, peginterferon, and ribavirin. Gastroenterology 2009;136 (3):856–862.

[31] Marcello T, Grakoui A, Barba-Spaeth G, Machlin ES, Kotenko SV, MacDonald MR, et al. Interferons alpha and lambda inhibit hepatitis C virus replication with distinct signal transduction and gene regulation kinetics. Gastroenterology 2006;131 (6):1887–1898.

[32] Robek MD, Boyd BS, Chisari FV. Lambda interferon inhibits hepatitis B and C virus replication. J Virol 2005;79 (6):3851–3854.

[33] McCarthy JJ, Li JH, Thompson A, Suchindran S, Lao XQ, Patel K, et al. Replicated association between an IL28B Gene Variant and a Sustained Response to Pegylated Interferon and Ribavirin. Gastroenterology 2010;138:2307–2314.

[34] Tanaka Y, Nishida N, Sugiyama M, Tokunaga K, Mizokami M. Λ-interferons and the single nucleotide polymorphisms: a milestone to tailor-made therapy for chronic hepatitis C. Hepatol Res 2010;40:449–460.

[35] Backus LI, Boothroyd DB, Phillips BR, Mole LA. Predictors of response of US veterans to treatment for the hepatitis C virus. Hepatology 2007;46 (1):37–47.

[36] Mori N, Imamura M, Kawakami Y, Saneto H, Kawaoka T, Takaki S, et al. Randomized trial of high-dose interferon-alpha-2b combined with ribavirin in patients with chronic hepatitis C: correlation between amino acid substitutions in the core/NS5A region and virological response to interferon therapy. J Med Virol 2009;81 (4):640–649.

[37] Hung CH, Lee CM, Lu SN, Lee JF, Wang JH, Tung HD, et al. Mutations in the NS5A and E2-PePHD region of hepatitis C virus type 1b and correlation with the response to combination therapy with interferon and ribavirin. J Viral Hepat 2003;10 (2):87–94.

[38] Yen YH, Hung CH, Hu TH, Chen CH, Wu CM, Wang JH, et al. Mutations in the interferon sensitivity-determining region (nonstructural 5A amino acid 2209–2248) in patients with hepatitis C-1b infection and correlating response to combined therapy of pegylated interferon and ribavirin. Aliment Pharmacol Ther 2008;27 (1):72–79.

[39] Zeuzem S, Lee JH, Roth WK. Mutations in the nonstructural 5A gene of European hepatitis C virus isolates and response to interferon alfa. Hepatology 1997;25 (3):740–744.

[40] Squadrito G, Leone F, Sartori M, Nalpas B, Berthelot P, Raimondo G, et al. Mutations in the nonstructural 5A region of hepatitis C virus and response of chronic hepatitis C to interferon alfa. Gastroenterology 1997;113 (2):567–572.

[41] Sarrazin C, Berg T, Lee JH, Teuber G, Dietrich CF, Roth WK, et al. Improved correlation between multiple mutations within the NS5A region and virological response in European patients chronically infected with hepatitis C virus type 1b undergoing combination therapy. J Hepatol 1999;30 (6):1004–1013.

[42] Murphy MD, Rosen HR, Marousek GI, Chou S. Analysis of sequence configurations of the ISDR, PKR-binding domain, and V3 region as predictors of response to induction interferon-alpha and ribavirin therapy in chronic hepatitis C infection. Dig Dis Sci 2002;47 (6):1195–1205.

[43] Pascu M, Martus P, Hohne M, Wiedenmann B, Hopf U, Schreier E, et al. Sustained virological response in hepatitis C virus type 1b infected patients is predicted by the number of mutations within the NS5A-ISDR: a meta-analysis focused on geographical differences. Gut 2004;53 (9):1345–1351.

[44] Thomas DL, Thio CL, Martin MP, Qi Y, Ge D, O'Huigin C, et al. Genetic variation in IL28B and spontaneous clearance of hepatitis C virus. Nature 2009;461 (7265):798–801.

[45] Kurosaki M, Enomoto N, Marumo F, Sato C. Evolution and selection of hepatitis C virus variants in patients with chronic hepatitis C. Virology 1994;205 (1):161–169.

[46] Enomoto N, Kurosaki M, Tanaka Y, Marumo F, Sato C. Fluctuation of hepatitis C virus quasispecies in persistent infection and interferon treatment revealed by single-strand conformation polymorphism analysis. J Gen Virol 1994;75 (Pt 6):1361–1369.

[47] Li JH, Lao XQ, Tillmann HL, Rowell J, Patel K, Thompson A, et al. Interferon-lambda genotype and low serum low-density lipoprotein cholesterol levels in patients with chronic hepatitis C infection. Hepatology 1904;51 (6):1904–1911.

[48] Serfaty L, Andreani T, Giral P, Carbonell N, Chazouilleres O, Poupon R. Hepatitis C virus induced hypobetalipoproteinemia: a possible mechanism for steatosis in chronic hepatitis C. J Hepatol 2001;34 (3):428–434.

ANTIMICROBIAL AGENTS AND CHEMOTHERAPY, June 2011, p. 2537–2545 Vol. 55, No. 6
0066-4804/11/$12.00 doi:10.1128/AAC.01780-10

Inhibitory Effect of a Triterpenoid Compound, with or without Alpha Interferon, on Hepatitis C Virus Infection▽†

Takako Watanabe,[1]‡ Naoya Sakamoto,[1,2]‡* Mina Nakagawa,[1,2] Sei Kakinuma,[1,2] Yasuhiro Itsui,[3] Yuki Nishimura-Sakurai,[1] Mayumi Ueyama,[1] Yusuke Funaoka,[1] Akiko Kitazume,[1] Sayuri Nitta,[1] Kei Kiyohashi,[1] Miyako Murakawa,[1] Seishin Azuma,[1] Kiichiro Tsuchiya,[1] Shinya Oooka,[1] and Mamoru Watanabe[1]

Department of Gastroenterology and Hepatology[1] and Department for Hepatitis Control,[2] Tokyo Medical and Dental University, Tokyo, Japan, and Department of Internal Medicine, Soka Municipal Hospital, Saitama, Japan[3]

Received 19 December 2010/Returned for modification 11 January 2011/Accepted 14 March 2011

A lack of patient response to alpha interferon (α-IFN) plus ribavirin (RBV) treatment is a major problem in eliminating hepatitis C virus (HCV). We screened chemical libraries for compounds that enhanced cellular responses to α-IFN and identified a triterpenoid, toosendanin (TSN). Here, we studied the effects and mechanisms of action of TSN on HCV replication and its effect on α-IFN signaling. We treated HCV genotype 1b replicon-expressing cells and HCV-J6/JFH-infected cells with TSN, with or without α-IFN, and the level of HCV replication was quantified. To study the effects of TSN on α-IFN signaling, we detected components of the interferon-stimulated gene factor 3 (ISGF3), phosphorylated signal transducer and activator of transcription 1 (STAT1), and STAT2 by Western blotting analysis; expression levels of mRNA of interferon regulatory factor 9 using real-time reverse transcription-PCR (RT-PCR); and interferon-stimulated response element reporter activity and measured the expression levels of interferon-inducible genes for 2′,5′-oligoadenylate synthetase, MxA, protein kinase R, and p56 using real-time RT-PCR. TSN alone specifically inhibited expression of the HCV replicon (50% effective concentration = 20.6 nM, 50% cytotoxic concentration > 3 μM, selectivity index > 146). Pretreatment with TSN prior to α-IFN treatment was more effective in suppressing HCV replication than treatment with either drug alone. Although TSN alone did not activate the α-IFN pathway, it significantly enhanced the α-IFN-induced increase of phosphorylated STATs, interferon-stimulated response element activation, and interferon-stimulated gene expression. TSN significantly increased baseline expression of interferon regulatory factor 9, a component of interferon-stimulated gene factor 3. Antiviral effects of treatment with α-IFN can be enhanced by pretreatment with TSN. Its mechanisms of action could potentially be important to identify novel molecular targets to treat HCV infection.

Hepatitis C virus (HCV) is one of the most important pathogens causing acute and chronic hepatitis, liver cirrhosis, and hepatocellular malignancies (29). Alpha interferon (α-IFN) combined with ribavirin (RBV) is the standard treatment for HCV infection (6, 10). However, virus elimination rates are about 50% among treated patients, and therapy is often accompanied by substantial side effects (6, 44). It was recently reported that genetic polymorphisms of the *IL28B* gene, which codes for lambda IFN, are critical for predicting responses to α-IFN plus RBV therapy (8, 35, 38). Patients with minor variants of *IL28B*, who comprise ~50% of Caucasian, 25% of Asian, and ~70% of African populations, showed poor responses to α-IFN treatment. Although new specific anti-HCV drugs are under development, many of them require combined use with α-IFN and RBV (26). Taken together, current difficulties in eliminating HCV are mostly attributable to the limited treatment options and to the limited activity of α-IFN against the virus. For this reason, the development of safe and effective agents that enhance antiviral actions against HCV has been a strong motivation in academia and industry.

To search for a new agent which enhances the effect of α-IFN, we used interferon-stimulated response element (ISRE) reporter screening. We screened a chemical library (60,500 compounds) for compounds that enhance ISRE activity when they are used in combination with α-IFN, using ISRE reporter screening, and identified several compounds that increased the ISRE reporter activities when they are used in combination with α-IFN and that did not show cytotoxicity. Among the hit compounds, toosendanin (TSN; $C_{30}H_{38}O_{11}$; molecular weight = 574) (Fig. 1), which is a triterpenoid derivative extracted from the bark of *Melia toosendan* Sieb et Zucc, was the strongest in enhancing α-IFN-induced ISRE reporter activation and the expression of interferon-stimulated genes (ISGs). TSN has been used as an anthelmintic vermifuge against ascaris (31). Although TSN has some other biological effects against toxin-producing anaerobic bacteria and against carcinoma cells (32, 45), antiviral activity has not been reported.

In this study, we showed, using an HCV replicon system, that TSN, with or without α-IFN, inhibits HCV replication in a cultured human hepatoma Huh7 cell line and that the combination of TSN and α-IFN shows synergistic effects on viral replication. We have investigated the mechanisms of action of

* Corresponding author. Mailing address: Department of Gastroenterology and Hepatology, Tokyo Medical and Dental University, 1-5-45 Yushima, Bunkyo-ku, Tokyo 113-8519, Japan. Phone: 81 3-5803-5877. Fax: 81 3-5803-0268. E-mail: nsakamoto.gast@tmd.ac.jp.

† Supplemental material for this article may be found at http://aac.asm.org/.

‡ T.W. and N.S. contributed equally to this work.

▽ Published ahead of print on 28 March 2011.

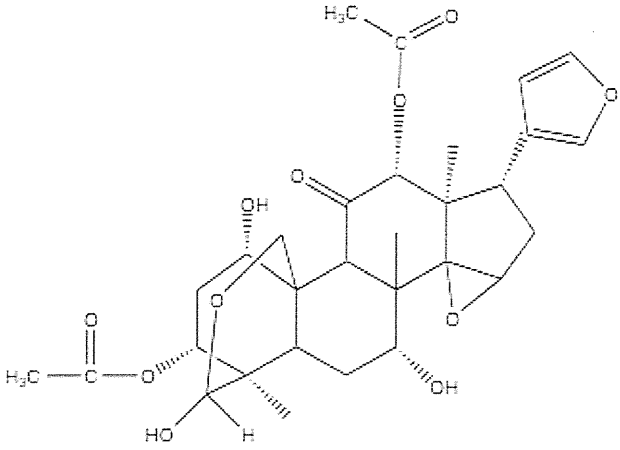

FIG. 1. Chemical structure of toosendanin.

TSN further and show that TSN induced activation of a component of interferon-stimulated gene factor 3 (ISGF3).

MATERIALS AND METHODS

Reagents. Alpha interferon was from Otsuka (Tokushima, Japan). TSN was from APIN Chemicals (Oxon, United Kingdom). Purity was over 77.32%. The designated concentration was achieved through dilution with cell culture medium (the final concentration of dimethyl sulfoxide [DMSO] in the medium was less than 0.3%). Beta-mercaptoethanol was from Wako (Osaka, Japan). The TSN used in this study was solubilized in DMSO.

Cells and cell culture. The human hepatoma cell line Huh7 was maintained in Dulbecco's modified Eagle's medium (Sigma, St. Louis, MO) supplemented with 10% fetal bovine serum at 37°C under 5% CO_2. To maintain cell lines carrying an HCV subgenomic replicon (Huh7/Rep-Feo), G418 (Nakalai Tesque, Kyoto, Japan) was added to the culture medium at a final concentration of 500 μg/ml.

HCV subgenomic replicon construct. The HCV subgenomic replicon plasmid pRep-Feo expresses a fusion gene comprising the firefly luciferase and neomycin phosphotransferase (37, 43). RNA was synthesized *in vitro* from the plasmid and transfected into Huh7 cells. After culture in the presence of G418, cell lines stably expressing the replicon were established.

Reporter constructs. We analyzed the effects of TSN, with or without α-IFN, on signal transduction of ISRE and nuclear factor-kappaB (NF-kappaB). A plasmid, pCIneo-Rluc-IRES-Fluc, was constructed to analyze HCV internal ribosome entry site (IRES)-mediated translation efficiency (23). Plasmids pISRE-TA-Luc and pNF-kappaB-Luc (Clontech Laboratories, Franklin Lakes, NJ) contained consensus motifs upstream of the firefly luciferase gene. A plasmid, pTA-Luc (Clontech), which lacks the enhancer element, was used to determine the background. Plasmid pRL-CMV (Promega, Madison, WI), which expresses the Renilla luciferase protein, was used for normalization of transfection efficiency (17).

ISRE reporter screening. Huh7 cells were seeded in 384-well plates at a density of 3.0×10^3 cells/well. An ISRE-responsive firefly luciferase reporter was introduced using Lipofectamine 2000 (Invitrogen). Five hours after transfection, the cells were treated with 60,500 compounds from chemical libraries at a concentration of 3 μg/ml for 24 h and then treated with α-IFN at a concentration of 3 IU/ml. Six hours later, cells were lysed, and luciferase activities were quantified using a Steady Glo luciferase assay kit (Promega). The compounds were stored in 100% DMSO, and thus, the final concentration of DMSO was 0.3%. *Z'* factors were calculated as reported previously (46).

Luciferase assays and measurements of antiviral activity. Huh7/Rep-Feo cells were cultured with various concentrations of compound, such that the final DMSO concentration was 0.1%. Levels of HCV replication were quantified by internal luciferase assay after 48 h of culture. Luciferase activities were quantified using a luminometer (Promega) and the Bright-Glo luciferase assay system (Promega). Assays were performed in triplicate, and the results are expressed as mean percentage of the controls ± standard deviation (SD). The 50% effective concentration (EC_{50}) values were calculated using the probit method (2, 33). The determination of EC_{50}s was performed three times, and EC_{50}s are presented as means ± SDs for each compound.

MTS assays. To evaluate cell viability, dimethylthiazol carboxymethoxyphenyl sulfophenyl tetrazolium (MTS) assays were performed using a Cell Titer 96 Aqueous One Solution cell proliferation assay (Promega) as previously reported (18, 22). Huh7/Rep-Feo cells and HCV-J6/JFH1-infected Huh7 cells were seeded in 96-well plates at a density of 8.0×10^3 cells/well. After treatment, to analyze the therapeutic index with the same concentration of the drug and administration time, 20 μl/well of Cell Titer 96 Aqueous One Solution reagent was added to the cells cultured in a 96-well plate, the plate was incubated at 37°C for 60 min, and then the absorbance at 490 nm was recorded with a 96-well plate reader. The cells were analyzed when the growth became confluent. Cell viability was expressed as the concentration required for 50% cytotoxicity (CC_{50}). The drug selectivity index was calculated as CC_{50}/EC_{50}. All experiments were performed in triplicate.

Analyses of drug synergism. The effects of treatment of Huh7/Rep-Feo cells with α-IFN, alone and in combination with TSN, were analyzed by using isobologram analysis as described previously (27, 37). Dose inhibition curves of α-IFN and TSN were drawn with the two drugs used alone or in combination. In each drug combination, EC_{50}s for α-IFN and TSN were plotted against the fractional concentration of α-IFN and TSN on the *x* and *y* axes, respectively. A theoretical line of additivity is drawn between plots of the EC_{50} for either drug that was used alone. The combined effects of the two drugs were considered additive, synergistic, or antagonistic if the plots of the drug combination were located on the line, below, or above the line of additivity, respectively.

HCV-J6/JFH1 cell culture. HCV-J6/JFH1 (21), which is a recombinant of HCV-JFH1 (42), was used. *In vitro*-synthesized HCV-J6/JFH1 RNA was transfected into naïve Huh7 cells (48), and the cells were cultured in the presence of drugs (34). Cellular viral RNA expression levels were measured using a real-time reverse transcription-PCR (RT-PCR) system.

Real-time RT-PCR analysis. Real-time RT-PCR was carried out as described previously (7). Total cellular RNA was extracted from cultured cells using Isogen (Nippon Gene, Tokyo, Japan), reverse transcribed, and subjected to real-time RT-PCR analyses. Expression of mRNA was quantified using TaqMan Universal PCR master mix, an ABI 7500 real-time PCR system (Applied Biosystems, CA), and a QuantiTect SYBR green PCR kit (Qiagen, CA). Some primers have been described elsewhere (30, 34). The primers used were -S (5′-TTT GAA ACA TCA AAG TTT TTC ACA GAC CTA-3′), -AS (5′-CAC AGT CAA GGT CCT TAG TAT TTC AGA TGT-3′), p56-S (5′-ACT TCG GAG AAA GGC ATT AGA TCT GGA AAG-3′), p56-AS (5′-TAA GGA CCT TGT CTC ACA GAG TTC TCA AAG-3′), Viperin-S (5′-GCT ACC AAG AGG AGA AAG CA-3′), Viperin-AS (5′-TTG ATC TTC TCC ATA CCA GC-3′), ISG20-S (5′-CTA CGA CAC GTC CAC TGA CAG G-3′), ISG20-AS (5′-CAT CGT TGC CCT CGC ATC TTC-3′), IRF9-S (5′-GCA GCA GCA GCC CTG AGC CAC AGG AAG TTA-3′), IRF9-AS (5′-TTA CCT GGA ACT TCG GTG GGG GGC CCA GGC-3′), IFNAR1-S (5′-CTT TCA AGT TCA GTG GCT CC-3′), IFNAR1-AS (5′-CAT CAG ATG CTT GTA CGC GGA G-3′), IFNAR2-S (5′-GCC AGA ATG CCT TCA TCG TCA G-3′), and IFNAR2-AS (5′-GTG AGT TGG TAC AAT GGA GTG G-3′).

Western blotting. Twenty micrograms of total cell lysate was separated by SDS-PAGE and blotted onto a polyvinylidene fluoride Western blotting membrane. The membrane was incubated with the primary antibodies, followed by incubation with a peroxidase-labeled anti-IgG antibody, and were visualized by chemiluminescence using an enhance chemiluminescence Western blotting analysis system (Amersham Biosciences, Buckinghamshire, United Kingdom). The antibodies used were mouse anti-NS5A (BioDesign, ME), rabbit anti-signal transducer and activator of transcription 1 (anti-STAT1) p84/p91, rabbit anti-phospho-STAT1 (Tyr 701), rabbit anti-STAT2, rabbit anti-phospho-STAT2 (Tyr 690) (Santa Cruz, CA), and anti-beta-actin antibody (Sigma). NIH image software was used to analyze the densitometry of the Western blot analysis. Quantification of STAT phosphorylation was done using NIH image software, and the results correspond to the ratio between the phosphorylated STAT1 (p-STAT1) or p-STAT2 amount and the STAT1 or STAT2 amount normalized to the amount for the control without α-IFN and TSN. The results correspond to the ratio between the NS5A amount and the beta-actin amount normalized to the amount for the control without α-IFN and TSN.

Statistical analyses. Statistical analyses were performed using Student's *t* test. *P* values of less than 0.05 were considered statistically significant.